NASA/TM-1999-209102

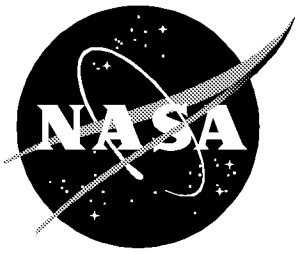

Air Force F-16 Aircraft Engine Aerosol Emissions Under Cruise Altitude Conditions

Bruce E. Anderson, W. Randy Cofer III, and David S. McDougal
Langley Research Center, Hampton, Virginia

March 1999

The NASA STI Program Office . . . in Profile

Since its founding, NASA has been dedicated to the advancement of aeronautics and space science. The NASA Scientific and Technical Information (STI) Program Office plays a key part in helping NASA maintain this important role.

The NASA STI Program Office is operated by Langley Research Center, the lead center for NASA's scientific and technical information. The NASA STI Program Office provides access to the NASA STI Database, the largest collection of aeronautical and space science STI in the world. The Program Office is also NASA's institutional mechanism for disseminating the results of its research and development activities. These results are published by NASA in the NASA STI Report Series, which includes the following report types:

- TECHNICAL PUBLICATION. Reports of completed research or a major significant phase of research that present the results of NASA programs and include extensive data or theoretical analysis. Includes compilations of significant scientific and technical data and information deemed to be of continuing reference value. NASA counterpart or peer-reviewed formal professional papers, but having less stringent limitations on manuscript length and extent of graphic presentations.

- TECHNICAL MEMORANDUM. Scientific and technical findings that are preliminary or of specialized interest, e.g., quick release reports, working papers, and bibliographies that contain minimal annotation. Does not contain extensive analysis.

- CONTRACTOR REPORT. Scientific and technical findings by NASA-sponsored contractors and grantees.

- CONFERENCE PUBLICATION. Collected papers from scientific and technical conferences, symposia, seminars, or other meetings sponsored or co-sponsored by NASA.

- SPECIAL PUBLICATION. Scientific, technical, or historical information from NASA programs, projects, and missions, often concerned with subjects having substantial public interest.

- TECHNICAL TRANSLATION. English-language translations of foreign scientific and technical material pertinent to NASA's mission.

Specialized services that complement the STI Program Office's diverse offerings include creating custom thesauri, building customized databases, organizing and publishing research results . . . even providing videos.

For more information about the NASA STI Program Office, see the following:

- Access the NASA STI Program Home Page at *http://www.sti.nasa.gov*

- Email your question via the Internet to help@sti.nasa.gov

- Fax your question to the NASA STI Help Desk at (301) 621-0134

- Telephone the NASA STI Help Desk at (301) 621-0390

- Write to:
  NASA STI Help Desk
  NASA Center for AeroSpace Information
  7121 Standard Drive
  Hanover, MD 21076-1320

NASA/TM-1999-209102

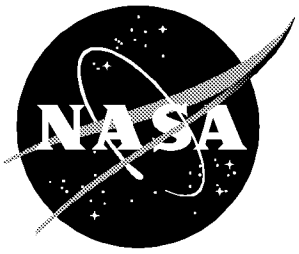

Air Force F-16 Aircraft Engine Aerosol Emissions Under Cruise Altitude Conditions

Bruce E. Anderson, W. Randy Cofer III, and David S. McDougal
Langley Research Center, Hampton, Virginia

National Aeronautics and
Space Administration

Langley Research Center
Hampton, Virginia 23681-2199

March 1999

Acknowledgments

We wish to thank the ground and flight crews of the Wallops T-39, in particular John Riley, for excellent support in conducting the SNIF-III mission and its difficult set of flight maneuvers and bumpy plume penetrations. We also express our gratitude to the Vermont and New Jersey Air National Guard Units for their enthusiastic support and participation.

Available from:

NASA Center for AeroSpace Information (CASI)
7121 Standard Drive
Hanover, MD 21076-1320
(301) 621-0390

National Technical Information Service (NTIS)
5285 Port Royal Road
Springfield, VA 22161-2171
(703) 605-6000

Contents

1. Summary

We documented results from the June 1997 Third Subsonic Assessment Near-Field Interactions Flight (SNIF-III) Experiment. The primary objectives of the SNIF-III experiment were to determine the partitioning and abundance of sulfur species and to examine the formation and growth of aerosol particles in the exhaust of F-16 aircraft as a function of atmospheric and aircraft operating conditions and fuel sulfur concentration. This information is, in turn, being used to address questions regarding the fate of aircraft fuel sulfur impurities and to evaluate the potential of their oxidation products to perturb aerosol concentrations and surface areas in the upper troposphere. SNIF-III included participation of the Vermont and New Jersey Air National Guard F-16's as source aircraft and the Wallops Flight Facility T-39 Sabreliner as the sampling platform. F-16's were chosen as a source aircraft because they are powered by the modern F-100 Series 220 engine, which is projected to be representative of future commercial aircraft engine technology. The T-39 instrument suite included sensors for measuring volatile and nonvolatile condensation nuclei (CN), aerosol size distributions over the range from 0.1 to 3.0 μm, 3-D winds, temperature, dewpoint, carbon dioxide (CO_2), sulfur dioxide (SO_2), sulfuric acid (H_2SO_4), and nitric acid (HNO_3). The experiment included a series of six flights which tested the influence of fuel sulfur content (FSC) on F-16 aircraft volatile aerosol emissions. On any particular flight, one F-16 burned standard JP-8 fuel (the same fuel used for all flights) whereas the other burned a Jet A mixture containing a low, medium, or high concentration of S impurities. (The same aircraft were in each flight.) For each fuel mixture, separate flights were performed at 30000- and 35000-ft altitudes to access a range of atmospheric temperatures, pressures, and moisture contents. In addition, the aircraft were sampled at two different power settings at each altitude to evaluate the effect of engine operating conditions upon trace species concentrations within the exhaust. Sampling was systematically performed at varying aircraft separations to access plume ages ranging from 0.2 to 20 sec.

The following text, tables, and figures summarize the aerosol observations recorded during SNIF-III and provide a more thorough description of the experiment and its rationale and objectives. A separate report will provide a summary of the wake/plume turbulence and mixing data recorded during SNIF-III, whereas information regarding the SO_2, H_2SO_4, and HNO_3 observations will appear in a later journal article.

2. Introduction

Because of concern that aviation-related emissions may have a detrimental effect on the global environment, NASA initiated a major research effort—the Subsonic Assessment (SASS)—aimed at characterizing what effect the current commercial aircraft fleet has on atmospheric chemical and radiative processes and what effect it may have in the coming years as air traffic increases. A portion of the SASS effort has concentrated upon characterizing and quantifying the direct particulate and gas phase emissions of aircraft at cruise altitudes and determining how exhaust plume chemistry and microphysics are influenced by interaction with the aircraft's trailing wingtip vortices. Of particular interest is determining the atmospheric fate of the sulfur contained as an impurity in jet fuel. Investigations focusing on these "near-field" concerns were solicited under NASA NRA 94-OA-01, and our group was selected to conduct an airborne investigation of aircraft aerosol emissions and wake/plume characteristics by using a small business-class jet (the Wallops T-39 Sabreliner), instrumented with fast response meteorological, trace gas, and aerosol sensors. To date, four successful flight series have been conducted, results from which have been discussed in numerous oral presentations and in peer-reviewed journal articles (Anderson et al., 1998a; 1998b; Miake-Lye et al., 1998). In addition to our suite of measurements, the group from Air Force Phillips Laboratory, headed by Dr. Al Viggiano, was funded under NRA-94-0A-01 to provide chemical ionization mass spectral (CIMS) measurements of gas phase sulfur species aboard the T-39 during the airborne investigations. Together, our groups instrumented the T-39 and, by participating in the Subsonic Assessment: Cloud and Contrail Effects Special Study (SUCCESS), conducted the highly successful SASS Near-field Interactions Flight (SNIF) Experiment series. Table 1 lists the dates, measurements, and types of aircraft sampled for the four missions (SNIF-I, SNIF-II, SUCCESS, and SNIF-III). Some general objectives for these missions were (1) to quantify (i.e., obtain emission indices for) the soot and volatile particle emissions of subsonic aircraft at cruise as a function of operational and atmospheric conditions; (2) to determine whether the

volatile particles seen in aircraft exhaust are composed of sulfur species; (3) to determine the partitioning of S in aircraft plumes between S(IV) and S(VI) species and to examine variations as a function of aircraft operating and environmental conditions; and (4) to obtain wake/plume dynamics measurements for model testing and validation.

The SNIF-I Experiment was conducted primarily to test the suite of instruments aboard the T-39 and to develop strategies for sampling within the turbulent wakes of much larger aircraft. During SNIF-II and SUCCESS, various aircraft plumes were sampled at altitudes ranging from the surface to 13 km, in contrail and noncontrail conditions, and at ages of 0.2 to 100 sec. Over 1000 plume crossings were accomplished. Aircraft at cruise were found to produce 0.5 to 10×10^{15} nonvolatile (presumably soot) particles kg^{-1} of fuel burned. These were typically 20 to 100 nm in diameter, and their numbers varied as a function of aircraft type and age along with engine operating parameters but not significantly with atmospheric conditions or plume age. In addition, high concentrations (emission indices of 0.1 to 40×10^{16} kg^{-1} fuel burned) of volatile aerosols were observed within all aircraft plumes. These particles were, except under contrail producing conditions, typically <20 nm in diameter, and their numbers varied as a function of atmospheric conditions, plume age, and fuel sulfur content. Their apparent hydrophilic nature and thermal characteristics are consistent with their being composed of condensed S species (Anderson et al., 1998b).

In order to further establish the volatile particle composition and to quantify the fraction of fuel sulfur released as S(VI) species for a typical commercial aircraft, we performed a carefully controlled fuel sulfur experiment during the 1996 SUCCESS campaign. The Langley B757 center and left wing tanks were fueled with Jet A containing ~70 ppm S whereas its right wing tank was filled with the same fuel containing an additive which brought its sulfur content up to ~700 ppm. The aircraft was flown in a racetrack pattern at cruise altitudes where it was followed closely by the T-39. The B757 alternated burning the low or high sulfur fuels in both engines or low sulfur fuel in the left engine and high sulfur fuel in the right. Average emission indices of $\sim 2 \times 10^{16}$ and 1×10^{15} volatile particles kg^{-1} of fuel burned were calculated for the high and low sulfur fuels, respectively. These values, coupled with concurrently recorded aerosol sizing information and gas phase sulfur measurements, indicated that 15 to 30 percent and 6 to 9 percent of the sulfur impurity in the high and low fuel S cases, respectively, were oxidized directly to sulfuric acid in the near-field behind the aircraft (for additional details, see Miake-Lye et al., 1998). These findings confirm that, as implied by the measurements of high volatile aerosol concentrations in the Concorde wake (Fahey et al., 1995), much higher concentrations of S(VI) species are generated by aircraft than can be accounted for by simple OH oxidation in the near-field plume. In addition, the observed increased efficiency of S(IV) oxidation to S(VI) at higher fuel S concentrations, as indicated by measurements of SO_2 in the exhaust plume, also conflicts with model predictions and suggests that additional (perhaps heterogeneous) mechanisms are required to account for the high levels of sulfuric acid seen in the aircraft plumes.

3. SNIF-III Experiment

3.1. Description

SNIF-III was conducted during May and June 1997 in collaboration with the Vermont (VANG) and the New Jersey Air National Guard (NJANG) Units located in Burlington and Atlantic City, respectively. In order to obtain a better understanding of fuel-S oxidation and particle formation and growth processes, the primary focus of the campaign was to obtain careful aerosol and sulfur species measurements in the exhaust of F-16 aircraft equipped with F-100 engines burning fuels with a range of fuel S concentrations at different altitudes and engine power settings. The F-100 engine was chosen both because it is anticipated to be representative of future commercial aircraft engine technology and because it was possible to obtain comparative measurements of trace gas and aerosol measurements behind one mounted in an altitude test cell at NASA Lewis Research Center (Wey et al., 1998). As shown in table 2, 10 missions were flown in which the exhaust plumes from 9 different F-16 aircraft were sampled.

Flights with VANG aircraft took place in restricted airspace over Vermont and New Hampshire whereas those with the NJANG took place in oceanic warning areas to the east of New Jersey and Delaware.

On flights 5, 6, 7, and 10, seven different aircraft burning either JP-8 or JP-8+100 were sampled at different altitudes, power settings, and separation distances (i.e., plume ages). Because these aircraft were selected at random and some had been refueled in-flight by tankers from different Guard Units, it was not possible to obtain fuel samples for sulfur analyses. Thus, these data are primarily useful for establishing differences in soot characteristics between standard military fuel and fuel containing the +100 additive that is supposed to reduce "coking" within the aircraft's afterburners.

The same pair of NJANG aircraft were sampled on the six missions conducted between June 25 and June 27. During these flights, one aircraft acted as a control, burning the same JP-8 fuel with 185 ± 17 ppm S in all cases, while the second aircraft burned a mixture containing either a high, medium, or low level of sulfur impurities. These latter fuels were obtained by purchasing two different batches of commercial Jet A fuel, one with the higher level of S (942 ± 38 ppm) and the other with low S (146 ± 34 ppm) content. The two fuels were then mixed to produce the medium S (527 + 14 ppm) fuel. Results of laboratory analyses of these fuels performed by the Air Force Lab in Bath, Maine, are shown in table 3. We note that the FSC's of the high and medium S fuels differ substantially from values reported by Wey et al. (1998) for the same fuels. Their tests, performed by Wright-Patterson Laboratory, indicate that the high and low S fuels contained 1113 ppm and 18 ppm S, respectively. The cause for these differences is unknown.

In order to meet specifications for use in Air Force F-16's, thermal conductivity, anti-corrosion, and anti-icing additives were mixed into the Jet A fuels before they were introduced into the aircraft. This process essentially converted the Jet A fuel to standard JP-8. In flight, the two aircraft were sampled under the same environmental and aircraft operating conditions so that the primary difference in emission characteristics could be related to the amount of sulfur in their fuels. Table 4 shows the test matrix followed in sampling the F-16's during flights 14, 15, 17, 18, 19, and 20. Two flights were conducted for each fuel mixture, one at 30000 ft and the second at 35000 ft or higher in order to characterize emissions in noncontrail and contrail forming conditions, respectively, and at different temperatures, pressures, and water vapor concentrations. During each flight, the source aircraft exhaust was sampled as a function of plume age (e.g., aircraft separation) at two different power settings, 78 percent and 88 percent at 30000 ft, and 78 percent and 85 percent at 35000 ft and higher.

3.2. Methods

The Wallops Flight Facility T-39 Sabreliner was used as the sampling platform (see fig. 1); it has a ceiling of 13 km, top speed of 0.8 Mach at cruise, and payload capability for carrying three standard racks of instruments, two pilots, and two observers. The aircraft has been modified with wing pylons to carry aerosol scattering spectrometer probes, radome pressure ports to provide vector airflow information, forward-looking video, and holes in the roof and belly for mounting sample inlets and optical devices. The aircraft also carries an inertial navigation and global positioning system receiver to provide platform motion in addition to pressure, temperature, and humidity sensors to establish altitude and ambient meteorological conditions.

The basic instrument suite, summarized in table 1, included a nondispersive infrared CO_2 analyzer, a passive cavity aerosol spectrometer probe, two ultrafine condensation nuclei counters (CNC's; TSI model 3025), and three standard condensation nuclei counters (TSI model 3760). A chemical ionization mass spectrometer was also flown to quantify plume concentrations of reactive gas phase nitrogen and sulfur species (Miake-Lye et al., 1998). In addition, a 24-channel aerosol impactor was flown to collect particle samples on copper grids for subsequent analyses by electron microscopy; results of these analyses will appear in a separate report. Inlets for these extractive-sampling instruments were located on the aircraft roof at approximately midship (fig. 2).

The CO_2 monitor was operated at a constant temperature and sample pressure. The monitor has a response time of ~5 Hz, a precision of 0.1 ppmv, and was calibrated periodically during each flight by using NOAA Environmental Research Laboratory standards. Both types of CNC's have ~1 Hz response time and are butanol-based and thus insensitive to particle solubility. Extensive laboratory characterizations and calibrations indicate that the ultrafine (UF) and fine (F) CNC's have 50 percent size cutoffs at 4 nm and 18 to 20 nm, respectively, when operated in the flight

configuration (Cofer et al., 1998; also see fig. 3). A third standard CNC was flown during SNIF-III and operated at a lower saturation temperature to obtain additional information on the size distribution of the volatile particles. To prevent saturating these instruments in the highly concentrated aircraft exhaust plumes, sample air was withdrawn from a sampling manifold through a critical flow orifice and immediately diluted by a factor of 10 to 50 with a concentric flow of filtered cabin air. This dilution provided the secondary benefit of allowing the CNC's to be operated at constant sample pressure and volumetric flow. The instruments are arrayed so that one each of the ultrafine and standard CNC's share a common inlet which can deliver a sample either at cabin temperature (~20°C) or can be heated to 300°C by passage through a 15-cm heat-tape wrapped tube. This arrangement allows quantification of total aerosols >4 nm and >20 nm, along with the number of nonvolatile, presumably soot particles and, by difference, volatile aerosols in the same size categories. Values for these parameters reported here have been corrected for the reduced efficiency of the CN counters at lower operating pressures and for particle losses within the inlet and sampling transport system.

The distance between the source and sampling aircraft was established in the following manner. The T-39 and collaborating Air National Guard F-16 aircraft carried air-to-air TACAN transceivers that provided a display of aircraft separation that was precise to about 100 m. Distances closer than 100 m were estimated by the pilots. Because the TACAN units did not provide an electronic output, distance information was called out periodically by the pilot over the aircraft intercom and written down as a function of time by the instrument operators. Because the aircraft separation was changing very slowly, this technique introduced only a slight additional error in precision.

Aerosol emission indices (EI), in terms of number of particles produced per kg fuel burned, were calculated from plume crossing data such as that shown in figure 4 by finding the enhancement ratios of aerosol species i to CO_2, dNi/dCO_2, and by assuming that the fuel combustion is 100 percent efficient. Jet fuel is nominally 86.3 percent carbon by weight, which produces an EI of 3160 g CO_2/kg fuel. Values of dNi/dCO_2 for individual plume crossings were calculated both by ratioing integrated peak areas (Fahey et al., 1995) and by linear regression analysis. Because the CO_2 and aerosol instruments had similar response times (see fig. 1), the two methods yielded similar results except in cases where the variability of CO_2 in the background air was comparable to its concentration change within the plume. These incidences were eliminated by limiting our analyses to only those cases which exhibited a >4 ppmv or 1 percent CO_2 enhancement above background levels. We estimate that the EI's presented below have an absolute accuracy of ±50 percent and a relative precision of ±20 percent.

3.3. Results

Tables 5 through 14 provide data for each of the 578 F-16 plume encounters that exhibited CO_2 enhancements of >4 ppmv and linear correlation coefficients between CO_2 and the aerosol species of interest of >0.7. The listed information includes source aircraft power settings (percent), plume crossing times, peak widths (sec), the flight altitudes (ft), ambient temperature (°C), temperature enhancements within the plumes (°C), ambient dewpoint (°C), peak CO_2 enhancements (ppmv), and emission indices for total ultrafine (UF), nonvolatile ultrafine (NUF), total fine (F), and nonvolatile fine (NF) particles (1×10^{15}/kg fuel burned). Plume ages are provided for most of the cases where the low, medium, and high S fuels were burned and in tables 6 and 7, which present data from flights in which more than one aircraft was sampled; the aircraft number is also given. Plume/Aircraft conditions presented in the tables for the 10 flights and 9 different source aircraft include power settings ranging from 70 percent to 100 percent with afterburners, altitudes from 23000 to 39000 ft, ambient temperatures from −19 to −60°C, dewpoints from −24 to −61°C, and CO_2 enhancements from 4 to 1900 ppmv.

Table 15 summarizes the data from tables 5 through 14. These summaries were prepared by sorting the data according to flight, aircraft, power setting, fuel type, and altitude and then by calculating statistics for the corresponding plume crossings. Values are presented for total number of crossings represented in the statistics along with the average altitudes, ambient temperatures, and dewpoints. In addition, averages, median values, and standard deviations are provided for the UF, NUF, F, and NF particle emission indices. In cases where the medium or high S fuels were

sampled, the statistics represent data from plumes which were >5 sec old.

3.3.1. Nonvolatile Particle Emissions

The data in tables 5 through 15 indicate that although there was a large degree of variability in the total aerosol emissions, nonvolatile particle emissions were relatively constant, except in the case where the aircraft afterburners were ignited. Histograms of NUF and NF aerosol EI's for the nonafterburner cases are shown in figures 5(a) and 5(b). Note that >60 percent of the cases exhibited NUF EI values between 2 and 4×10^{15} kg^{-1} fuel burned and that the extremes in the data set differed only by a factor of 4. The NF EI's were even less variable, with 95 percent of the values lying between 1 and 2.5×10^{15} kg^{-1} fuel burned. Both histograms, however, exhibit somewhat bimodal characters, with the NUF plot showing a clear secondary peak between 4.5 and 5×10^{15} kg^{-1}.

To investigate the cause of the skewness in the figure 5 distributions further, we examine the emission characteristics of the individual F-16's sampled during SNIF-III. Figure 6 provides statistics for the VANG F-16's burning JP-8+100 fuel (aircraft 1 through 5) and the NJANG aircraft (6 through 9) burning fuels meeting the standard JP-8 specifications. With the exception of aircraft 6, the VANG aircraft clearly show higher EI's than the NJANG F-16's. Indeed, mean values of NUF and NF EI's for the VANG aircraft are $5.0 \pm 2.1 \times 10^{15}$ kg^{-1} and $2.3 \pm 0.6 \times 10^{15}$ kg^{-1}, respectively, whereas those for the NJANG F-16's, including aircraft 6, are $3.0 \pm 1.0 \times 10^{15}$ kg^{-1} and $1.5 \pm 0.7 \times 10^{15}$ kg^{-1}, respectively. The ~60 percent higher EI's for the Vermont aircraft cannot be related to differences in power settings or environmental factors because these, as discussed below, caused only slight changes in the F-16 nonvolatile aerosol emissions and, in any case, were approximately the same for both series of flights. Thus, we surmise that the differences are related to slight variations in the age or maintenance history of engines on the Vermont and New Jersey F-16's or to differences in combustion properties of the JP-8 and JP-8+100 fuels. Because engine data were not collected on the individual aircraft, none of the possible explanations can be ruled out. We note, however, that the +100 additives were introduced to the JP-8 fuels specifically to alter engine aerosol emission characteristics.

Besides fuel, other parameters that varied during the SNIF-III flight series include time since engine maintenance, engine power setting, altitude, and plume age. Figure 7 shows the flight by flight nonvolatile aerosol emissions of the NJANG F-16 used in the fuel sulfur study. The aircraft had undergone regular maintenance just before flight 14 and accumulated ~1.5 hr run time per flight for a total of ~9 hr over the course of the experiment. Over this period, the NUF emissions show no systematic trend whereas the NF EI's exhibit a slight decrease with time.

The effect of engine power setting upon F-16 nonvolatile aerosol emission is illustrated in figure 8, a plot prepared from the data of table 6. NF EI values vary <20 percent at powers <100 percent and only increase slightly when the aircraft afterburners are engaged. Conversely, NUF emissions are relatively constant at or below 90 percent power but increase 30 to 40 fold at 100 percent power. We speculate that a majority of the NUF particles seen in the afterburner case were unburned fuel residue which could not be volatilized to <4 nm diameter particles during the short passage through our inlet heater.

Figure 9 shows that all NUF and NF EI values obtained during the mission were plotted as a function of altitude. The slightly greater EI's at the mid to lower altitudes are caused by inclusion of the VANG data. These aircraft, noted previously to produce ~60 percent more aerosol emissions than the NJANG F-16's, were not sampled above 11 km, so the apparent decrease in NUF emissions at the highest altitude is related to this factor. In addition, the ratio of NF to NUF EI's is relatively constant with altitude, indicating that the particle size distributions are relatively unaffected.

As expected, the nonvolatile aerosol emission characteristics did not vary as a function of plume age or dilution. Figure 10 presents all NUF and NF EI's from the NJANG JP-8 control aircraft recorded on flights 14 through 20 plotted as a function of peak CO_2 enhancement, which is representative of plume dilution. Both parameters vary randomly across the factor of 500 change in plume concentration.

3.3.2. Total Particle Emissions

In contrast to their relatively invariant nonvolatile aerosol emissions, the F-16's total particle emissions, particularly for the UF component, varied

considerably as a function of each study parameter. Figure 11 shows a random distribution plot of UF and F EI's for the mission. Values range from 1 to ~900×10^{15} and from <1 to 4×10^{15} kg^{-1} fuel burned for UF and F, respectively. The F points are clustered between 1 and 4×10^{15} kg^{-1} fuel burned, which indicates that in a majority of cases, the nonvolatile component accounted for most of the particles >18 nm in diameter (see fig. 5(b)). Indeed, the only F EI values >5×10^{15} kg^{-1} correspond to times when the aircraft pilot applied afterburners to maneuver into position or climb (i.e., see table 8, crossings 22 through 27) or in response to our request (see table 6, crossings 109 through 117). At these times, the aircraft is essentially exhausting unburned jet fuel. This unburned fuel has a profound effect upon all but the NF component of the aerosol (see fig. 12). By examining the tables and flight notes, we conclude that for the UF component, all values >2.4×10^{17} kg^{-1} correspond to afterburner cases.

Results from the SUCCESS mission indicated that FSC played a major role in controlling aircraft total aerosol emissions (Anderson et al., 1998b; Miake-Lye et al., 1998). Figures 13(a) and 13(b) summarize results from the six flights conducted in collaboration with the NJANG in which fuels with three levels of FSC were burned in a single F-16. The data are from plumes >5 sec old and the multiple points shown for most flights represent data recorded at different power settings or altitudes. For example, the three flight 18 data points correspond to statistics for the 35000-ft low and high power setting data (table 10, crossings 1 through 20 and 21 through 28, respectively) and the 38000-ft plumes (table 10, crossings 62 through 77), respectively. Figure 13(a) shows that UF particle EI's were significantly higher than NUF EI's for both the medium and high FSC fuels but were roughly equal in the case of low FSC. Measurements recorded behind the "control" F-16 burning standard JP-8 fuel with FSC of ~170 ppm S (figs. 14(a) and 14(b)) provide confidence that the variations in UF EI portrayed in figure 13(a) are not due to variations in engine parameters (e.g., maintenance or operating conditions) or to environmental factors. Thus, because the fuels were identical in all other aspects, we can only conclude that the volatile aerosol fraction is comprised of oxidized sulfur species. Because the F EI's are not significantly enhanced at the higher FSC levels (fig. 13(b)) we can also surmise that a majority of the volatile particles are <18 nm in diameter.

In addition, our observations suggest that either volatile particle production is a nonlinear function of FSC or that FSC must exceed a certain threshold before the particles grow to exceed the 4-nm diameter cutoff point of our UF CN counters. For example, while the S levels of the medium and high S fuels differed by only a factor of two, the UF EI's for the high FSC cases were on average eight times greater than for the medium FSC plumes. Also, although the low S and JP-8 fuels contained >15 percent as much S as the high S fuel, they produced only slight average plume enhancements of volatile UF (see figs. 15(a) and 15(b)).

In the high and medium S cases, the data points of figure 13(a) show a fair amount of variability at constant FSC. Factors observed to create this variability include plume age, flight altitude, and contrail formation; engine power setting does not appear to play a significant role (see figs. 16(a) and 16(b)). Figures 17(a) through 17(h) show UF EI's plotted as a function of plume age for the high and medium S cases of tables 10 through 12 where aircraft separation data were available. In the case shown in figure 16(a) (high FSC, 80 percent engine power at 35000 ft altitude), the IE was ~1.5×10^{16} kg^{-1} fuel burned at a plume age of 0.5 sec and increased by an order of magnitude over the ensuing 5 sec. As shown in figure 18, corresponding NUF, F, and NF EI's remained approximately constant over the time interval. Figures 17(b) through 17(h) show features similar to figure 17(a), although the growth rate appears to be somewhat slower for the medium FSC and contrail cases. We expect that the primary process being observed in these time series plots is not the formation of new particles, but rather growth of particles formed a few meters downstream of the engines to sizes measurable by our UF CN counter.

The growth and perhaps lifetime of the aerosol nuclei are apparently very sensitive to environmental conditions. Figure 19 shows UF EI data recorded behind the NJANG F-16 as it burned the medium S fuel at flight altitudes of 30000, 35000, and 37000 ft, the latter altitude in heavy contrail forming conditions. Values at 5-sec plume age decreased by a factor of three in going from 30000 to 35000 ft and dropped an additional ~50 percent between 35000 and 37000 ft. Exhaust plume CN number densities are often reduced within contrails by deposition onto the much larger ice crystals, thus the low observed EI's at 37000 ft are not

surprising. However the difference between the 30000- and 35000-ft legs is not easily explained. UF EI data obtained behind the F-16 as it burned high FSC fuel did not show a similar trend. Indeed, the data of table 10 suggest that values actually increase with altitude. Speculation for the UF EI behavior in the medium FSC cases include that the relative humidity was high enough at 35000 ft to create subvisible contrails or that particle growth mechanisms at this FSC level are particularly sensitive to environmental factors.

4. Concluding Remarks

We have documented cruise-altitude aerosol emissions from a number of Air Force F-16 fighter-jet aircraft, all using the same model F-100 Series 220 engines. Total and nonvolatile EI's for ultrafine and fine aerosols are presented for different fuels and as a function of engine power, flight altitude, plume age, and varying environmental conditions. Results indicate that nonvolatile aerosol EI's from the nine aircraft sampled during SNIF-III were rather tightly distributed between 1 and 6×10^{15} kg^{-1} fuel burned. The values were also relatively insensitive to aircraft operating parameters (other than use of afterburners) and environmental factors but may have varied somewhat with aircraft maintenance history or fuel formulations. Afterburner use did not affect NF EI's but enhanced NUF EI's by one to two orders of magnitude, presumably by introducing droplets of unburned hydrocarbons into the exhaust stream which could not be evaporated to <4 nm diameter within our short sample inlet heater.

In contrast to the nonvolatile aerosol components, total aerosol EI's from the F-16's were highly variable, ranging from near 1×10^{15} to almost 1×10^{18} kg^{-1} fuel burned. Although all independent flight parameters had some influence on total aerosol emissions, afterburner use was the most effective, being responsible for all cases where F and UF EI's exceeded 1×10^{16} and 2.4×10^{17} kg^{-1} fuel burned, respectively. Indeed it was the only observed means of generating significant numbers of volatile particles in the exhaust of aircraft burning fuels with <200 ppm S content.

Under normal operating conditions, FSC was the primary factor which regulated total aerosol emissions from the aircraft. For example, whereas fuel with ~146 ppm S produced an insignificant number of volatile UF particles, the 942 ppm S fuel resulted in UF EI's almost two orders of magnitude higher than those for NUF. The medium S fuel (527 ppm) produced UF EI's which were only 10 to 20 percent as great as those in the high FSC cases, indicating that either the formation of sulfur-based particles is a highly nonlinear function of FSC or that the FSC must exceed a certain threshold before particles grow to exceed the lower size cutoff our UF CN counter. For a given FSC, the plume age and, particularly for the medium fuel S cases, environmental conditions played significant roles in regulating observed UF EI's.

NASA Langley Research Center
Hampton, VA 23681-2199
November 5, 1998

5. References

Anderson, B. E.; Cofer, W. R.; Bagwell, D. R.; Barrick, J. W.; Hudgins, C. H.; and Brunke, K. E.: Airborne Observations of Aircraft Aerosol Emissions, I—Total Nonvolatile Particle Emission Indices. *Geophys. Res. Lett.*, vol. 25, no. 10, 1998, pp. 1689–1692.

Anderson, B. E.; Cofer, W. R.; Barrick, J. D.; Bagwell, D. R.; and Hudgins, C. H.: Airborne Observations of Aircraft Aerosol Emissions, II—Factors Controlling Volatile Particle Production. *Geophys. Res. Lett.*, vol. 25, no. 10, 1998, pp. 1693–1696.

Cofer, W. R., III; Anderson, B. E.; Winstead, E. L.; and Bagwell, D. R.: Calibration and Demonstration of a Condensation Nuclei Counting System for Airborne Measurements of Aircraft Exhausted Particles. *Atmos. Environ.*, vol. 32, no. 2, 1998, pp. 169–177.

Fahey, D. W.; Keim, E. R.; Boering, K. A.; Brock, C. A.; Wilson, J. C.; et al.: Emission Measurements of the Concorde Supersonic Aircraft in the Lower Stratosphere. *Science*, vol. 270, no. 5233, 1995, pp. 70–74.

Miake-Lye, R. C.; Anderson, B. E.; Cofer, W. R.; Wallio, H. A.; Nowicki, G. D.; et al.: SOx Oxidation and Volatile Aerosol in Aircraft Exhaust Plumes Depend on Fuel Sulfur Content. *Geophys. Res.* Lett., vol. 25, no. 10, 1998, pp. 1677–1680.

Wey, C. C.; Wey, C.; Dicki, D. J.; Loos, K. H.; Noss, D. E.; et al.: *Engine Gaseous, Aerosol Precursor and Particulate at Simulated Flight Altitude Conditions*. NASA TM-1998-208509, 1998.

Table 1. Near Field Flight Experiments Conducted Aboard the Wallops T-39

Mission	SNIF-1	SNIF-II	SUCCESS	SNIF-III
Dates	Jul-95	Jan/Feb-96	Apr/May-96	May/Jun-97
Number of flights	5	8	16	20
T,Tdew	No	Yes	Yes	Yes
CO_2	Yes	Yes	Yes	Yes
3-D winds	No	Yes	Yes	Yes
CN > 4 nm	Yes	Yes	Yes	Yes
CN > 18 nm	Yes	Yes	Yes	Yes
CN > 25 nm	No	No	No	Yes
CN > 100 nm	No	Yes	Yes	Yes
SO_2, H_2S0_4	No	Partial	Partial	Yes
HNO_3, HONO	No	Partial	Partial	Yes
CN composition	No	No	No	Yes
Source Aircraft	B-737, T-39	B-737, T-38, T-39, B747, MD-80	B-757, DC-8, B-727	B-737, BE-200, C-130, F-16

Table 2. SNIF-III Flights To Sample F-16 Exhaust Plumes

Flight number	Flight date	T-39 takeoff	T-39 landing	Number of source A/C	Aircraft affiliation	Fuel type
5	6/6/98	1700	1850	1	NJANG	JP-8
6	6/9/97	1400	1540	3	VANG	JP-8+100
7	6/9/97	1800	1930	1	VANG	JP-8+100
10	6/13/97	1550	1740	1	NJANG	JP-8
14	6/25/97	1330	1530	2	NJANG	JP-8/Jet A w/high S
15	6/25/97	1800	2000	2	NJANG	JP-8/Jet A w/high S
17	6/26/97	1315	1510	2	NJANG	JP-8/Jet A w/medium S
18	6/26/97	1725	1930	2	NJANG	JP-8/Jet A w/medium S
19	6/27/97	1320	1520	2	NJANG	JP-8/Jet A w/low S
20	6/27/97	1730	1910	2	NJANG	JP-8/Jet A w/low S

Table 3. Characteristics of the Fuels Used During the SNIF-III Fuel Sulfur Experiment

Fuel type	Fuel canister	Analysis number	Sample date	Fuel S PpmM	Fuel sample identity
JP-8	97-F-1333	9700765	13-Jun-97	208	Control F-16 fuel from refueler
Jet A	97-F-953	9700780	16-Jun-97	1000	High sulfur content fuel
Jet A	97-F-975	9700832	20-Jun-97	<500	Low sulfur content fuel
Jet A	97-F-1211	9700867	25-Jun-97	926	High sulfur fuel from F-16
Jet A	97-F-1014	9700868	25-Jun-97	921	High sulfur fuel from F-16
JP-8	97-F-1015	9700869	25-Jun-97	172	Control F-16 fuel
JP-8	97-F-1206	9700865	25-Jun-97	180	Control F-16 fuel
JP-8	97-F-1015	9700869	25-Jun-97	172	Control F-16 fuel
Jet A	97-F-1016	9700880	26-Jun-97	923	High sulfur fuel from F-16
Jet A	97-F-1019	9700883	26-Jun-97	516	Medium S fuel mixture from F-16
Jet A	97-F-1017	9700884	26-Jun-97	524	Medium S fuel mixture from F-16
JP-8	97-F-1018	9700885	26-Jun-97	167	Control F-16 fuel
JP-8	97-F-1134	9700881	26-Jun-97	192	Control F-16 fuel
JP-8	97-F-1335	9700886	26-Jun-97	207	Control F-16 fuel
Jet A	97-F-1336	9700887	26-Jun-97	543	Medium S fuel mixture from F-16
JP-8	97-F-1207	9700900	27-Jun-97	101	Low sulfur content fuel from F-16
Jet A	97-F-1208	9700903	27-Jun-97	170	Low sulfur content fuel from F-16
Jet A	97-F-1102	9700901	27-Jun-97	118	Low sulfur content fuel from F-16
JP-8	97-F-1103	9700902	27-Jun-97	170	Low sulfur content fuel from F-16
JP-8	97-F-1104	9700904	27-Jun-97	174	Low sulfur content fuel from F-16

Table 4. Test Matrix for the SNIF-III Fuel S Flights

Fuel sulfur	Low	Medium	High
Environmental parameters	T, P, Q (altitude)	T, Q, P (altitude)	T, Q, P (altitude)
Aircraft parameters	78%–88% power	78%–88% power	78%–88% power
Aircraft separation Distance 30 meters + + + + + + 2 km			

Table 5. Flight 5, New Jersey F-16

(a) Standard JP-8 Fuel+A23

Power setting, percent	Crossing number	Plume crossing time			Peak width, sec	Altitude, ft	Ambient temperature, °C	Temperature enhancement, °C	Ambient dewpoint, °C	Plume enhancement, ppmv	Emission indices (1×10^{15} kg)			
		Hr	Min	Sec							UF	NUF	F	NF
83	1	17	42	27	13	23323	−19.8	0.87	−25.9	37.1	5.8	5.2	2.1	1.9
83	2	17	42	58	31	23514	−20.2	1.24	−28.5	78.5		5.9	2.4	2.3
83	3	17	43	46	27	23702	−20.5	1.84	−28.6	71.4	6.0	5.6	2.6	2.3
83	4	17	44	6	11	23722	−20.5	0.52	−28.4	44.4	5.9	5.8	2.7	2.2
83	5	17	44	43	6	23871	−21.0	0.32	−28.9	20.7	6.5	6.0	2.8	1.7
83	6	17	45	41	5	24267	−22.0	0.06	−30.5	27.5	6.3	5.5	2.6	1.4
83	7	17	45	54	4	24040	−21.7	0.20	−30.4	54.8	6.2	5.4	2.5	1.3
83	8	17	46	20	30	24317	−22.1	1.69	−25.6	77.8	6.0	5.6	2.5	2.2
83	9	17	47	28	9	25560	−25.8	0.73	−30.0	38.7	5.1	4.7	2.5	2.0
83	10	17	48	13	8	26563	−28.1	1.17	−33.2	42.3	5.2	5.3	2.1	1.8
83	11	17	48	38	37	27879	−31.1	3.27	−33.9	103.4	5.2	4.7	2.2	2.0
83	12	17	49	18	42	28750	−33.5	3.45	−36.4	106.0	5.5	5.4	2.3	2.3
83	13	17	49	47	10	29034	−34.2	1.03	−37.3	65.8	4.9	4.7	2.2	2.0
78	14	17	50	2	9	29358	−35.2	1.21	−38.4	66.5	5.1	4.7	2.1	1.9
78	15	17	50	37	16	29515	−36.0	0.40	−40.8	23.0	5.9	5.8	2.2	2.2
78	16	17	50	53	8	29508	−35.8	0.32	−41.2	30.5	6.5	6.5	2.3	2.2
78	17	17	51	20	6	29281	−35.4	0.39	−42.0	22.0	5.6	6.1	2.0	1.9
78	18	17	52	48	8	29176	−35.0	0.50	−39.2	8.8	5.3	4.5	2.2	2.0
78	19	17	53	0	12	29418	−35.5	0.70	−39.6	9.2	5.1	4.9	2.1	2.2
78	20	17	53	19	14	29609	−36.1	1.09	−40.7	51.0	6.7	6.9	2.4	2.3
78	21	17	53	35	14	29633	−36.3	0.77	−41.0	49.0	5.6	5.5	2.4	2.2
78	22	17	53	59	7	29782	−36.6	0.08	−40.8	5.1	5.5	5.3	1.9	1.7
78	23	17	54	15	24	29831	−36.5	1.35	−39.9	103.8	6.4	5.8	2.5	2.3
78	24	17	54	41	9	29864	−36.7	1.13	−39.6	82.3	5.5	5.8	2.3	2.2
78	25	17	55	38	97	30158	−37.4	3.03	−38.5	246.8	6.1	5.6	2.3	2.3
78	26	17	56	34	8	30061	−37.4	0.91	−39.7	63.1	6.6	6.1	2.3	2.2
78	27	17	57	20	38	30190	−37.5	1.47	−40.5	131.7	6.1	5.7	2.3	2.4

Table 5. Concluded

(b) Standard JP-8 Fuel

Power setting, percent	Crossing number	Plume crossing time			Peak width, sec	Altitude, ft	Ambient temperature, °C	Temperature enhancement, °C	Ambient dewpoint, °C	Plume enhancement, ppmv	Emission indices (1×10^{15} kg)			
		Hr	Min	Sec							UF	NUF	F	NF
78	28	17	57	58	20	30110	−37.3	1.11	−38.1	132.8	6.0	5.4	2.3	2.1
78	29	17	58	22	26	29965	−37.0	1.09	−39.4	103.6	5.5	4.6	2.1	1.8
70	30	18	2	1	10	30313	−37.9	0.93	−38.4	39.7	5.4	4.7	2.2	1.8
70	31	18	2	55	24	28635	−34.0	2.70	−39.8	9.5	52.4	2.7	0.9	0.8
70	32	18	3	11	5	28394	−33.2	0.42	−38.5	11.4	97.8	4.2	1.0	0.8
70	33	18	3	37	6	26999	−29.0	0.78	−35.1	25.3	36.1	3.6	1.0	0.8
70	34	18	6	25	22	23840	−21.3	0.59	−26.6	25.4	6.1	5.8	2.6	2.4
70	35	18	6	44	6	23890	−21.6	0.22	−26.6	5.1	7.0	8.0	3.1	2.7
70	36	18	7	16	7	23803	−21.4	0.35	−27.7	26.5	5.7	5.8	2.6	2.3
70	37	18	7	25	8	23818	−21.5	0.43	−27.3	25.6	5.3	5.5	2.7	2.4
70	38	18	7	43	26	23822	−21.5	0.65	−25.7	46.1	6.2	5.6	2.8	2.5
70	39	18	8	6	3	23853	−21.6	0.67	−26.1	26.8	3.8	4.9	2.0	2.6
90	40	18	9	0	8	23643	−21.0	0.25	−26.6	28.9	5.2	5.0	2.3	2.1
90	41	18	9	23	6	23782	−21.5	0.35	−27.0	23.6	5.2	5.9	2.4	1.9
90	42	18	9	46	6	23794	−21.7	0.89	−25.7	66.5	4.6	3.9	1.8	1.3
90	43	18	9	54	6	23823	−21.7	0.82	−25.5	56.0	4.3	3.5	1.9	1.4
90	44	18	10	8	15	23851	−21.9	0.96	−26.4	62.8	4.8	4.4	1.9	1.7
90	45	18	10	29	24	23946	−21.9	1.11	−26.8	67.4	4.3	3.8	1.9	1.5
90	46	18	10	56	29	24005	−21.9	1.24	−26.7	81.1	4.3	4.1	1.9	1.6
90	47	18	11	15	7	23962	−21.9	1.23	−26.6	71.6	4.2	3.9	1.8	1.4
90	48	18	11	28	10	23911	−21.8	1.01	−27.0	62.6	4.8	4.0	1.9	1.6
90	49	18	12	15	7	23942	−21.8	0.63	−26.9	48.5	5.0	3.6	1.9	1.5
90	50	18	12	33	7	24008	−21.8	0.48	−26.8	32.6	4.8	4.1	1.8	1.5
90	51	18	12	53	8	23954	−21.7	0.52	−26.6	55.7	5.9	3.5	1.8	1.5
90	52	18	13	14	7	24038	−21.9	0.86	−26.6	52.0	4.7	3.1	1.7	1.4
90	53	18	13	36	21	24090	−21.5	1.00	−26.5	57.9	4.6	3.3	1.8	1.5
90	54	18	13	58	19	24170	−21.7	1.18	−26.3	61.6	7.0	4.4	1.9	1.6

Table 6. Flight 6, Vermont F-16's With JP-8+100 Fuel

Aircraft power, percent	Crossing number	Plume crossing time			Peak width, sec	Altitude, ft	Ambient temperature, °C	Temperature enhancement, °C	Ambient dewpoint, °C	Plume enhancement, ppmv	Emission indices (1×10^{15} kg)			
		Hr	Min	Sec							UF	NUF	F	NF
#1/78	2	14	22	52	4	30144	−40.4	0.16	−50.8	11.1	6.4	4.8	1.8	1.1
#1/78	3	14	24	15	6	29724	−39.4	0.23	−52.2	35.7	6.4	4.4	1.9	1.7
#1/78	4	14	24	31	13	29733	−39.5	1.16	−52.4	56.6	5.3	3.7	1.7	1.9
#2/78	5	14	26	42	10	29959	−40.1	1.13	−52.2	58.9	5.8	5.5	2.3	2.7
#2/78	6	14	26	58	5	29868	−39.9	0.70	−52.1	43.3	6.3	4.8	2.7	2.2
#2/78	7	14	27	5	8	29899	−40.0	0.85	−52.0	57.9	5.2	4.7	2.4	2.5
#2/78	8	14	27	17	14	29987	−40.2	1.17	−51.9	64.0	6.7	5.3	2.4	2.5
#2/78	9	14	27	34	5	29905	−40.2	0.41	−51.7	12.5	6.8	4.7	2.2	2.2
#2/78	10	14	28	1	8	29843	−39.7	0.74	−51.8	37.4	6.7	4.6	2.6	2.8
#2/78	11	14	28	21	8	29794	−39.8	0.87	−52.0	40.4	6.9	4.4	2.3	2.2
#2/78	12	14	28	33	8	29785	−39.8	0.58	−52.1	44.6	8.0	4.8	2.4	2.5
#2/78	13	14	28	48	5	29832	−40.1	1.00	−52.1	52.5	7.4	4.3	2.3	2.2
#2/78	14	14	28	58	6	29813	−40.0	0.66	−52.2	37.8	9.5	5.0	2.0	2.0
#2/78	15	14	29	13	12	29913	−40.3	1.10	−52.2	41.3	10.4	7.1	2.1	2.4
#2/78	16	14	29	25	9	29854	−40.1	1.08	−52.0	37.2	9.8	5.4	2.3	2.5
#2/78	17	14	29	44	8	29916	−40.0	0.67	−51.4	48.9	7.7	6.1	2.3	2.6
#3/78	18	14	30	15	10	29647	−39.4	1.07	−50.5	14.3	613.0	24.7	48.4	1.3
#3/78	19	14	30	35	7	29787	−39.6	0.99	−49.9	77.1	207.0	6.5	3.6	3.2
#3/78	20	14	30	46	10	29838	−39.7	0.87	−49.5	57.6	368.0	7.8	51.5	2.5
#3/78	21	14	31	9	35	29882	−40.1	1.28	−47.4	70.0		7.3		2.9
#3/78	22	14	31	36	7	29867	−39.9	0.79	−47.5	42.4	73.4	6.0	2.4	2.6
#3/78	23	14	31	46	7	29982	−40.1	0.39	−47.9	12.7	69.3	5.2	2.4	2.6
#3/78	24	14	32	0	12	30022	−40.1	0.58	−48.7	50.7	37.6	5.9	2.7	2.8
#3/78	25	14	32	28	9	29905	−40.1	0.32	−49.5	29.3	35.2	6.2	2.8	3.1
#3/78	26	14	32	38	5	29924	−40.2	0.36	−49.5	14.8	15.8	5.4	2.6	3.0
#3/78	27	14	32	45	6	29944	−40.1	0.79	−49.5	46.8			2.5	2.4
#3/78	28	14	32	53	5	30029	−40.2	0.59	−49.3	30.0	36.6	5.9	2.7	2.4
#3/78	29	14	33	0	6	29953	−39.9	0.94	−49.1	42.7	62.1	8.5	2.7	2.4
#3/78	30	14	33	30	7	30081	−40.5	0.61	−48.6	24.3	53.9	6.1	3.0	2.9

Table 6. Continued

Aircraft power, percent	Crossing number	Plume crossing time			Peak width, sec	Altitude, ft	Ambient temperature, °C	Temperature enhancement, °C	Ambient dewpoint, °C	Plume enhancement, ppmv	Emission indices (1×10^{15} kg)			
		Hr	Min	Sec							UF	NUF	F	NF
#1/88	31	14	36	55	10	29918	–40.2	0.81	–49.6	59.3	11.2	3.8	1.8	1.9
#1/88	32	14	37	16	8	29965	–40.3	0.65	–49.2	46.5	9.2	3.3	1.8	1.8
#1/88	33	14	37	25	8	30030	–40.4	1.26	–49.0	60.8	10.3	3.5	1.8	1.8
#1/88	34	14	37	56	12	30063	–40.6	0.75	–49.2	44.6	9.3	4.0	1.8	2.0
#1/88	35	14	38	12	7	30119	–40.7	0.66	–49.5	37.9	9.9	3.3	1.8	1.7
#1/88	36	14	38	41	7	30054	–40.8	0.39	–50.2	46.2	8.4	3.5	1.9	1.7
#1/88	37	14	39	2	6	29984	–40.8	0.09	–50.6	8.6	10.0	3.9	1.7	1.8
#1/88	38	14	39	17	5	30042	–41.4	1.06	–50.8	23.1	6.3	3.9	1.7	1.9
#1/88	39	14	39	24	5	29971	–40.6	0.88	–50.9	37.5	8.8	3.9	2.0	1.7
#2/88	40	14	40	50	15	29886	–40.0	1.42	–49.2	161.0	7.0	4.8	2.5	2.4
#2/88	41	14	41	34	31	29905	–40.1	2.42	–45.8	141.3	8.2	4.6	2.3	2.5
#2/88	42	14	41	54	7	29939	–40.3	1.23	–45.9	66.3	7.9	5.6	2.1	2.0
#2/88	43	14	42	3	7	29945	–40.3	1.16	–46.4	74.1	8.9	4.1	2.2	2.0
#2/88	44	14	42	10	8	29958	–40.7	1.49	–47.3	45.7	9.3	4.8	2.2	2.2
#2/88	45	14	42	34	9	29929	–40.2	0.92	–49.2	62.6	8.6	4.8	2.1	2.3
#2/88	46	14	42	46	12	29920	–40.0	1.19	–49.7	77.6	9.0	4.0	2.2	1.8
#2/88	47	14	43	2	8	29868	–40.0	1.12	–49.5	58.6	8.9	4.3	2.0	1.8
#2/88	48	14	43	18	7	29865	–39.9	0.55	–49.0	53.6	5.9	3.8	2.0	1.9
#3/88	49	14	44	49	11	29666	–39.4	2.32	–47.9	113.5	129.0	7.8	2.6	1.9
#3/88	50	14	45	3	7	29673	–39.1	1.40	–47.4	52.7			1.7	2.0
#3/88	51	14	45	32	16	29878	–39.8	3.13	–47.6	205.3	26.1	5.2	2.7	2.8
#3/88	52	14	45	48	15	29855	–39.8	3.74	–47.2	221.3	24.9	5.2	2.6	2.7
#3/88	53	14	46	10	27	29875	–39.9	1.60	–47.6	101.3	33.8	4.8	2.4	2.3
#3/88	54	14	46	46	43	29858	–40.3	1.32	–47.9	74.4	0.0	5.3	2.5	2.7
#3/88	55	14	47	21	15	29955	–40.7	1.16	–48.7	57.1	35.7	4.6	2.5	2.4
#3/88	56	14	47	38	5	30059	–40.9	0.33	–49.4	12.3	109.0	5.7	3.1	2.3
#1/78	57	14	56	0	4	35173	–51.0	0.22	–56.6	20.6	110.0	3.3	1.7	0.8
#1/78	58	14	56	12	7	35122	–50.9	0.30	–56.6	11.4	96.6	5.2	1.8	1.8
#1/78	59	14	56	20	4	35145	–51.1	0.24	–56.6	10.5	46.9	3.2	2.3	1.4
#1/78	60	14	56	28	5	35125	–51.2	0.39	–56.5	16.8	31.3	3.5	2.2	1.8
#1/78	61	14	56	34	5	35142	–51.3	0.37	–56.5	16.3	34.4	3.8	2.2	1.6
#1/78	62	14	56	41	6	35025	–51.1	0.39	–56.5	17.7	29.0	4.2	2.1	1.7
#1/78	63	14	56	52	11	35023	–50.8	0.65	–56.3	32.1	14.7	3.1	2.3	1.9
#1/78	64	14	57	3	8	34862	–50.6	0.61	–56.0	34.0	26.5		2.4	2.0

Table 6. Continued

Aircraft power, percent	Crossing number	Plume crossing time			Peak width, sec	Altitude, ft	Ambient temperature, °C	Temperature enhancement, °C	Ambient dewpoint, °C	Plume enhancement, ppmv	Emission indices (1×10^{15} kg)			
		Hr	Min	Sec							UF	NUF	F	NF
#1/78	65	14	57	32	9	34656	−50.1	1.39	−55.6	85.6	29.4	3.8	2.3	1.8
#1/78	66	14	57	56	39	34676	−50.4	2.66	−53.9	152.4	35.7	4.3	2.4	2.3
#1/78	67	14	58	22	10	34697	−50.5	0.87	−53.4	56.6	36.2	4.3	2.4	2.2
#1/85	68	14	59	40	12	34774	−51.0	0.40	−55.4	15.3	15.6	4.0	2.4	2.3
#1/85	69	15	0	6	10	34643	−50.9	0.85	−55.3	11.7	11.3	4.9	2.4	2.2
#1/85	70	15	1	41	7	34258	−49.7	0.34	−54.3	16.5		4.7	2.1	2.3
#1/85	71	15	1	52	9	34193	−49.7	0.99	−54.3	26.2	6.5	3.5	2.0	1.9
#1/85	72	15	2	3	6	33899	−48.8	0.61	−54.3	46.9	11.0	5.7	2.2	2.0
#2/78	74	15	4	16	8	34467	−50.1	1.91	−54.7	40.7	9.5	4.1	2.7	2.1
#2/78	75	15	4	23	4	34527	−50.3	0.22	−54.6	29.5	17.5	4.0	2.2	2.0
#2/78	76	15	4	31	6	34676	−50.4	0.85	−54.5	40.5	5.8	5.3	3.2	2.5
#2/78	77	15	4	41	12	34810	−50.7	0.94	−54.4	39.9	8.6	4.9	2.8	2.3
#2/78	78	15	4	51	6	34707	−50.7	0.31	−54.4	36.3		6.1	2.7	2.5
#2/78	79	15	5	8	20	34916	−51.0	0.75	−54.4	30.6	7.2	5.5	2.9	2.8
#2/78	80	15	5	36	8	34851	−50.9	0.89	−54.8	11.8	6.2	5.3	2.9	2.6
#2/78	81	15	5	47	7	34840	−51.0	0.15	−55.1	5.8	69.8	1.4	1.1	0.8
#2/78	82	15	5	56	6	34837	−52.0	1.21	−55.3	8.6	7.7	4.6	3.0	2.6
#2/78	83	15	6	17	10	34886	−50.8	0.37	−55.9	17.9		5.4	3.0	3.0
#3/78	84	15	7	50	28	35186	−51.3	5.65	−50.8	280.9	13.1	5.3	2.5	2.0
#3/78	85	15	8	22	35	35020	−50.6	0.76	−55.1	48.5	10.8	5.4	2.9	2.5
#3/78	86	15	8	46	9	34935	−50.7	0.76	−55.7	39.1	11.1	5.0	3.0	2.8
#3/78	87	15	9	1	20	34927	−50.7	1.20	−55.8	35.0	10.7	5.4	3.0	3.2
#3/78	88	15	9	27	32	34634	−50.7	0.73	−53.9	34.8		7.1	4.2	3.4
#3/78	89	15	10	3	15	34621	−50.6	0.51	−53.0	18.5	44.7	5.5	3.3	3.1
#3/78	90	15	10	24	21	34794	−50.6	0.57	−53.3	20.4	43.4	5.5	3.4	2.9
#3/78	91	15	10	43	13	34887	−50.7	0.69	−53.9	24.1	29.5	6.0	3.2	3.0
#3/78	92	15	12	17	10	34544	−49.9	1.03	−54.2	65.1	8.2	3.9	2.7	2.4
#3/78	93	15	12	30	11	34579	−50.0	1.18	−54.0	60.0	10.3	3.4	2.7	2.4

Table 6. Concluded

Aircraft power, percent	Crossing number	Plume crossing time			Peak width, sec	Altitude, ft	Ambient temperature, °C	Temperature enhancement, °C	Ambient dewpoint, °C	Plume enhancement, ppmv	Emission indices (1×10^{15} kg)			
		Hr	Min	Sec							UF	NUF	F	NF
#3/100	94	15	12	38	5	34600	–50.3	0.29	–53.9	30.3	12.3	4.7	2.8	3.0
#3/100	95	15	12	46	4	34623	–50.5	0.16	–53.8	8.3	39.6	7.5	3.4	2.3
#3/100	96	15	12	52	6	34615	–50.5	0.78	–53.7	44.3	16.3	4.8	3.0	2.7
#3/100	97	15	12	59	5	34620	–50.4	0.14	–53.6	16.1	47.2	4.8	3.0	
#3/100	98	15	13	6	6	34677	–50.6	0.59	–53.6	27.2	57.8	5.9	3.1	2.6
#3/100	99	15	13	14	6	34639	–50.6	0.59	–53.6	27.4	32.7	4.8	3.3	2.7
#3/100	100	15	13	27	7	34752	–50.6	0.73	–53.6	29.3	17.1	5.0	3.1	2.8
#3/100	101	15	13	33	4	34755	–50.8	0.31	–53.6	31.0	10.3	4.9	3.0	2.8
#3/100	102	15	13	38	5	34810	–51.0	0.78	–53.7	29.6	10.9	5.1	3.1	2.6
#3/100	103	15	13	45	5	34842	–51.1	0.55	–53.7	27.2	8.5	4.4	3.2	2.5
#3/100	104	15	13	54	5	34825	–50.9	0.34	–53.8	17.4	9.0	4.2	3.2	2.7
#3/100	105	15	14	1	6	34838	–51.8	1.25	–53.9	19.0	9.1	6.1	3.6	2.7
#3/100	106	15	14	16	6	35052	–51.3	0.79	–54.4	30.2	6.3	4.5	3.0	2.4
#3/aftb	109	15	14	48	5	35386	–51.9	0.29	–54.6	10.6	866.0	92.4	410.0	1.7
#3/aftb	110	15	15	0	15	35123	–51.6	0.58	–54.9	24.1	816.0	92.6	347.0	2.1
#3/aftb	111	15	15	14	11	34898	–51.0	0.92	–54.9	51.0	500.0	76.0	251.0	0.9
#3/aftb	112	15	15	23	6	34825	–50.8	0.80	–54.8	49.7	453.0	50.9	199.0	
#3/aftb	113	15	15	32	5	34821	–51.0	1.11	–54.6	22.1	630.0	142.0	348.0	1.6
#3/aftb	114	15	15	38	7	34795	–51.0	0.49	–54.4	27.2	594.0	107.0	299.0	1.7
#3/aftb	115	15	15	47	6	34720	–50.8	0.15	–54.3	13.2	547.0	32.7	102.0	4.2
#3/aftb	116	15	15	55	7	34659	–51.7	1.38	–54.1	23.5	659.0	41.8	211.0	4.2
#3/aftb	117	15	16	7	7	34722	–51.2	0.78	–53.9	24.1	649.0	38.3	158.0	4.3

Table 7. Flight 7, Vermont F-16's With JP-8+100 Fuel

Aircraft power, percent	Crossing number	Plume crossing time			Peak width, sec	Altitude, ft	Ambient temperature, °C	Temperature enhancement, °C	Ambient dewpoint, °C	Plume enhancement, ppmv	Emission indices (1×10^{15} kg)			
		Hr	Min	Sec							UF	NUF	F	NF
#4/88	2	18	34	23	17	29587	–38.4	1.23	–41.9	55.4		4.2	1.6	1.5
#4/88	3	18	34	49	12	29525	–38.2	0.55	–43.4	41.0	62.9	3.5	0.0	1.6
#4/78	4	18	35	2	7	29401	–37.7	0.65	–44.1	46.0	24.3	3.2	1.3	1.4
#4/78	5	18	35	22	23	29380	–37.6	0.81	–43.2	51.8		3.2	1.6	1.6
#4/78	6	18	35	44	6	29485	–37.8	0.52	–41.7	26.1	15.3	4.2	1.5	1.6
#4/78	7	18	35	53	9	29469	–38.0	0.82	–40.9	34.4	11.9	3.9	1.6	1.8
#4/78	8	18	36	13	5	29677	–38.4	0.39	–40.7	12.3	18.2	4.3	1.9	1.6
#4/78	9	18	36	49	10	29758	–38.9	0.37	–42.2	19.4	11.9	3.7	1.9	2.0
#5/78	10	18	46	55	29	30076	–39.8	0.93	–41.4	42.3	7.3	4.3	1.9	2.0
#5/78	11	18	47	12	5	30017	–39.3	0.61	–41.3	47.7	6.1	4.9	2.3	2.2
#5/78	12	18	47	18	5	30020	–39.5	0.58	–41.1	44.6	6.3	4.4	2.7	3.2
#5/78	13	18	47	30	12	30003	–39.4	1.04	–41.0	103.9		5.4	2.6	2.7
#5/78	14	18	47	45	11	29984	–39.4	0.52	–41.0	76.9	5.4	3.9	2.5	1.9
#5/78	15	18	48	10	23	29946	–39.3	1.34	–40.8	66.4	6.7	4.9	2.4	2.3
#5/78	16	18	48	25	5	29754	–39.1	0.38	–40.7	50.6	4.7	4.0	2.5	2.2
#5/78	17	18	48	47	9	29801	–39.1	0.99	–41.1	54.2	9.5	6.8	3.5	3.1
#5/88	18	18	49	6	9	29884	–39.3	0.86	–41.9	47.2	15.7	4.9	2.9	2.8
#5/88	19	18	49	18	8	29724	–39.0	0.85	–42.4	49.7	36.9	4.7	2.5	2.2
#5/88	20	18	49	30	13	29673	–38.8	1.00	–42.5	54.1	48.8	5.9	2.6	2.2
#5/88	21	18	49	40	6	29746	–38.9	1.18	–42.4	56.4	16.3	4.3	2.3	2.2
#5/88	22	18	49	48	8	29839	–38.9	0.47	–42.4	15.2	22.8	5.2	2.6	2.6
#5/88	23	18	50	5	22	29861	–38.9	1.18	–42.9	55.9	11.7	4.1	2.4	2.2
#5/88	24	18	50	19	7	29860	–39.1	1.23	–43.2	49.9	12.8	4.9	2.5	2.4
#4/78	25	18	56	41	37	34592	–49.7	1.80	–53.2	47.8	4.7	4.0	2.1	2.1

Table 8. Flight 10, New Jersey F-16 With Standard JP-8 Fuel

Power setting, percent	Crossing number	Plume crossing time			Peak width, sec	Altitude, ft	Ambient temperature, °C	Temperature enhancement, °C	Ambient dewpoint, °C	Plume enhancement, ppmv	Emission indices (1×10^{15} kg)			
		Hr	Min	Sec							UF	NUF	F	NF
83	2	16	14	40	18	29310	−32.4	1.53	−47.2	107.9	3.0	3.0	2.1	1.6
83	3	16	14	58	17	29311	−32.4	1.57	−47.2	100.7		2.9	2.2	1.6
83	4	16	15	15	11	29399	−32.6	1.63	−47.1	94.3	3.1	2.8	2.1	1.7
83	5	16	15	39	21	29346	−32.9	0.90	−46.8	83.0	2.8	2.7	2.1	1.6
83	6	16	16	22	10	29375	−32.9	0.87	−39.0	45.7	2.9	3.0	2.1	1.6
83	7	16	16	43	5	29338	−33.0	0.57	−41.5	87.9	2.2	2.3	1.8	1.1
83	8	16	17	8	11	29513	−33.0	0.89	−35.7	67.7	2.8	3.1	2.1	1.5
83	9	16	17	34	6	29412	−32.3	0.33	−35.7	56.1	2.6	2.6	1.9	1.5
83	10	16	17	51	11	29507	−32.4	0.94	−36.6	67.0	3.0	3.2	1.9	1.4
83	11	16	18	7	6	29371	−32.2	0.98	−34.9	84.9	3.0	3.3	1.9	1.4
83	12	16	18	25	10	29365	−31.9	0.59	−35.0	41.6		3.4	1.7	1.2
78	13	16	19	28	7	28233	−30.6	0.90	−34.2	60.3	1.9	2.2	1.2	1.1
78	14	16	21	46	11	27174	−27.3	0.85	−44.4	49.1	3.0	2.9	2.1	1.7
90	15	16	22	30	23	27830	−29.0	3.21	−39.5	198.4	2.4	2.3	1.7	1.4
90	16	16	22	53	17	28187	−29.8	2.30	−43.3	125.2	2.3	2.3	1.6	1.3
90	17	16	23	10	16	28529	−30.8	1.88	−46.0	109.2	3.1	2.7	1.6	1.3
90	18	16	23	58	20	29464	−33.1	1.06	−43.9	78.6		2.2	1.5	1.2
90	19	16	24	17	15	29630	−33.4	1.49	−38.2	88.6	2.8	2.6	1.7	1.5
90	20	16	24	55	13	30245	−35.2	1.00	−43.7	51.8	2.5	2.3	1.7	1.3
90	21	16	25	20	14	31006	−36.5	1.44	−37.4	45.9	2.8	2.7	1.8	1.3
85	22	16	35	12	8	36174	−51.4	0.30	−52.4	15.5	470.0	17.7	80.0	3.3
85	23	16	35	34	6	36417	−52.0	0.33	−53.4	11.5	93.5	4.0	3.1	1.7
85	24	16	45	9	12	37445	−54.8	1.10	−58.2	70.1	237.0	25.3	110.0	5.8
85	25	16	55	31	9	38900	−58.5	0.19	−62.2	7.6	558.0	26.6	287.0	1.7
85	26	16	55	45	7	38800	−58.5	0.22	−61.4	5.7	408.0	27.8	220.0	2.1
85	27	16	55	55	9	38973	−58.7	0.58	−60.7	8.9	301.0	32.6	126.0	2.5
85	28	16	56	35	8	39185	−59.1	0.49	−59.9	17.6	4.2	3.9	2.6	1.8
85	29	16	56	50	16	39108	−59.3	0.64	−60.5	17.2	2.5	2.8	2.2	1.5
85	30	16	57	4	10	39016	−58.8	0.38	−60.8	11.6		1.7	2.0	1.4
85	31	16	57	17	12	38885	−58.7	0.62	−60.9	21.1		3.6	2.8	1.7
85	32	16	57	28	7	38786	−58.6	0.54	−60.9	20.4	1.1	2.8	2.2	1.6
85	33	16	57	39	14	38824	−58.9	0.78	−60.7	29.6	3.5	3.2	3.2	1.9
85	34	16	57	53	11	38779	−58.6	0.32	−60.3	29.1	3.2	3.6	2.8	1.9
85	35	16	58	6	14	38596	−58.2	0.88	−59.8	42.5	4.4	3.4	2.9	1.7

Table 8. Concluded

Power setting, percent	Crossing number	Plume crossing time			Peak width, sec	Altitude, ft	Ambient temperature, °C	Temperature enhancement, °C	Ambient dewpoint, °C	Plume enhancement, ppmv	Emission indices (1×10^{15} kg)			
		Hr	Min	Sec							UF	NUF	F	NF
85	36	16	58	21	9	38701	–58.2	1.69	–59.3	97.3	121.0	31.5	69.3	11.5
85	37	16	58	30	7	38781	–58.5	2.08	–59.0	98.6		16.0		
85	38	16	58	39	7	38609	–58.1	0.55	–58.7	27.3	208.0	31.3	113.0	3.4
85	39	16	58	52	8	38593	–58.1	0.44	–58.6	28.6	164.0	23.7	77.1	2.8
85	40	16	59	4	9	38680	–58.1	0.72	–58.8	25.7				2.6
85	41	16	59	11	4	38858	–58.2	0.43	–59.0	13.8	2.9	2.0	2.4	0.0
85	42	16	59	24	10	38976	–58.4	0.67	–59.4	30.2	2.7	2.6	2.3	1.7
85	43	16	59	38	12	38975	–58.5	0.56	–59.7	22.4	2.4	2.4	2.3	1.5
85	44	17	0	12	47	39460	–59.5	0.99	–60.9	20.8	3.0	2.7	2.2	1.5
85	45	17	0	46	7	39322	–59.5	0.33	–60.4	14.6	1.7	2.1	1.8	1.1
85	46	17	0	59	19	39274	–59.5	0.52	–59.6	14.3		2.3	1.8	1.4

Table 9. Flight 14, New Jersey F-16

(a) High Sulfur Content Fuel

Power setting, percent	Crossing number	Plume crossing time			Peak width, sec	Altitude, ft	Ambient temperature, °C	Temperature enhancement, °C	Ambient dewpoint, °C	Plume enhancement, ppmv	Emission indices (1×10^{15} kg)			
		Hr	Min	Sec							UF	NUF	F	NF
88	1	14	30	4	10	30399	–33.0	1.0	–45.4	107.7	87.2	4.0	1.8	1.5
88	2	14	30	15	10	30375	–32.8	1.3	–45.7	135.5	86.9	4.3	1.9	1.6
88	3	14	38	44	7	30506	–33.5	0.2	–47.5	36.4	17.5	2.5	1.2	1.2
88	4	14	38	54	10	30493	–33.3	2.2	–47.2	553.6	20.5	3.3	1.3	1.3
88	5	14	39	5	10	30505	–33.4	0.1	–46.8	110.8	39.1	3.2	1.4	1.4
88	6	14	39	22	23	30429	–33.0	4.6	–43.9	403.6	39.1	2.8	1.4	1.3
88	7	14	40	47	8	30524	–33.2	3.2	–46.2	270.6	53.5	3.8	1.4	1.3
88	8	14	40	57	8	30505	–33.2	0.1	–45.6	13.0	140.0	4.2	1.5	1.4
88	9	14	41	16	9	30473	–33.1	0.3	–44.9	30.5	137.0	3.7	1.6	1.4
88	10	14	41	31	5	30508	–33.2	0.2	–45.2	3.1	168.0	3.5	1.4	1.5
88	11	14	41	41	11	30420	–33.0	0.6	–45.4	53.2	136.0	3.5	1.7	1.6
88	12	14	41	56	9	30435	–33.1	0.8	–45.5	46.2	165.0	3.7	1.6	1.6
88	13	14	42	6	10	30430	–33.2	1.1	–45.8	47.2	169.0	4.1	1.6	1.6

Table 9. Concluded

(b) Standard JP-8 Fuel

Power setting, percent	Crossing number	Plume crossing time			Peak width, sec	Altitude, ft	Ambient temperature, °C	Temperature enhancement, °C	Ambient dewpoint, °C	Plume enhancement, ppmv	Emission indices (1×10^{15} kg)			
		Hr	Min	Sec							UF	NUF	F	NF
80	15	14	46	30	8	30381	−33.1	0.91	−47.1	72.4	2.1	2.2	1.3	1.4
80	16	14	48	15	20	30310	−33.0	1.11	−47.1	57.0	2.0	1.8	1.3	1.2
80	17	14	48	34	6	30377	−33.2	0.53	−46.9	36.3	3.3	2.6	1.3	1.2
80	18	14	49	20	9	30413	−33.1	0.13	−46.1	10.6	2.2	1.9	1.4	1.2
80	19	14	49	59	16	30511	−33.3	1.73	−44.6	77.4	2.1	2.1	1.3	1.3
90	20	14	50	18	7	30390	−33.1	1.13	−44.3	59.7	2.3	2.3	1.2	1.2
90	21	14	52	6	23	30464	−32.3	13.29	−38.9	1847.9	1.8	1.8	1.0	1.0
90	22	14	53	50	13	30481	−33.2	1.06	−50.0	64.5	2.8	2.1	1.3	1.3
90	23	14	54	12	14	30459	−33.2	1.18	−44.1	57.6	2.0	1.8	1.4	1.2
90	24	14	54	34	10	30470	−33.2	1.59	−41.9	75.3	2.8	1.9	1.4	1.3
90	25	14	55	7	13	30464	−33.1	0.77	−46.0	50.8	2.0	2.0	1.3	1.3
90	26	14	55	27	10	30479	−33.2	0.89	−46.5	48.5	2.2	2.0	1.3	1.3
90	27	14	55	42	13	30427	−33.0	0.65	−45.5	42.5	2.1	2.0	1.4	1.4
90	28	14	56	29	8	30366	−33.2	0.39	−47.8	31.8	2.5	1.9	1.4	1.3
90	29	14	56	39	10	30335	−33.0	0.46	−48.9	32.3	2.1	1.7	1.3	1.2
90	30	14	56	50	7	30345	−33.1	0.42	−49.5	32.8	2.0	1.9	1.2	1.2

Table 10. Flight 15, New Jersey F-16

(a) High Sulfur Content Fuel

Power setting, percent	Crossing number	Plume crossing time			Peak width, sec	Altitude, ft	Plume age	Ambient temperature, °C	Temperature enhancement, °C	Ambient dewpoint, °C	Plume enhancement, ppmv	Emission indices (1×10^{15} kg)			
		Hr	Min	Sec								UF	NUF	F	NF
80	1	18	41	39	8	35472	0.5	–45.8	0.3	–56.5	321.1	13.7	2.3	1.6	1.3
80	2	18	41	54	21	35417	0.9	–45.7	1.4	–56.4	336.7	18.2	2.3	1.6	1.4
80	3	18	42	15	18	35383	0.9	–45.6	1.4	–56.0	312.1	31.9	2.5	1.9	1.6
80	4	18	42	31	11	35370	1.4	–45.4	2.6	–55.2	204.3	51.5	2.5	1.8	1.5
80	5	18	42	59	27	35421	1.8	–45.5	1.9	–50.0	121.1	75.3	2.6	1.8	1.6
80	6	18	43	21	15	35295	2.3	–45.5	0.8	–51.8	63.8	87.6	2.8	1.9	1.6
80	7	18	43	34	11	35289	2.3	–45.3	0.6	–53.0	46.5	101.5	2.6	1.8	1.5
80	8	18	43	52	22	35212	2.7	–45.1	0.8	–54.2	53.4	97.1	2.9	1.8	1.5
80	9	18	45	10	11	35358	1.8	–45.6	0.8	–54.1	46.6	85.9	2.8	2.0	1.6
80	10	18	45	26	9	35329	2.7	–45.4	0.8	–53.4	56.0	96.5	2.8	1.8	1.5
80	11	18	45	42	5	35336	2.7	–45.5	0.1	–53.3	14.9	118.3	2.8	2.3	1.5
80	12	18	45	57	7	35319	2.7	–45.4	0.3	–53.6	43.5	95.9	2.1	1.8	1.4
80	13	18	46	26	10	35274	3.6	–45.2	0.6	–54.0	43.4	94.3	2.6	2.2	1.5
80	14	18	46	38	11	35272	4.5	–44.8	1.3	–54.0	44.8	105.4	2.7	1.8	1.4
80	15	18	46	46	3	35246	5.4	–45.3	0.1	–54.0	4.5	149.5	1.5	3.6	0.7
80	16	18	47	6	10	35275	6.3	–45.5	0.5	–54.0	15.8	143.9	2.8	2.3	1.5
80	17	18	47	34	7	35392	7.2	–45.7	0.4	–53.9	14.8	170.1	3.1	1.8	1.6
80	18	18	47	51	25	35373	8.1	–45.5	0.5	–53.6	21.7	161.2	2.5	2.1	1.8
80	19	18	48	11	14	35434	9.0	–45.5	0.9	–53.6	25.7	151.7	3.1	2.0	1.8
80	20	18	49	6	16	35216	9.0	–45.4	0.8	–53.7	23.0	147.8	2.6	2.0	1.6
85	21	18	53	29	50	35499	0.5	–44.8	7.4	–42.6	423.8	21.5	2.6	1.7	1.6
85	22	18	53	59	9	35483	0.9	–45.2	3.6	–46.6	265.5	30.6	2.8	1.8	1.3
85	23	18	54	11	6	35519	0.9	–45.2	1.4	–49.5	159.2	39.6	2.6	1.9	1.5
85	24	18	54	17	4	35519	0.9	–45.4	0.1	–50.8	25.4	41.0	3.2	1.6	2.2
85	25	18	54	32	26	35507	1.4	–43.1	2.2	–55.4	156.7	53.9	2.9	2.2	1.9
85	26	18	55	0	29	35318	1.8	–45.1	1.9	–57.8	123.9	73.6	2.9	2.1	1.8
85	27	18	55	30	8	35324	2.3	–45.2	0.5	–58.7	62.6	82.0	3.2	2.2	1.6
85	28	18	55	39	8	35258	2.7	–44.9	0.8	–58.9	70.9	83.7	3.5	2.2	1.7

Table 10. Continued

(a) Concluded

Power setting, percent	Crossing number	Plume crossing time			Peak width, sec	Altitude, ft	Plume age	Ambient temperature, °C	Temperature enhancement, °C	Ambient dewpoint, °C	Plume enhancement, ppmv	Emission indices (1×10^{15} kg)			
		Hr	Min	Sec								UF	NUF	F	NF
88	29	18	56	6	5	35252	3.6	−45.0	0.7	−59.4	33.7	116.0	3.9	2.0	1.6
88	30	18	58	28	8	35241	4.5	−45.3	0.9	−59.4	32.6	126.6	2.9	2.0	1.6
88	31	18	58	38	10	35282	5.0	−45.4	0.6	−59.3	32.4	119.9	2.7	2.0	1.8
88	32	18	58	46	5	35218	5.4	−45.2	0.4	−59.2	30.5	107.1	2.7	2.0	1.6
88	33	18	58	57	10	35218	5.4	−45.1	1.0	−59.1	34.7	94.8	3.6	2.0	1.7
88	34	18	59	20	7	35343	7.2	−45.5	0.4	−58.7	21.9	184.6	3.0	2.3	1.6
88	35	18	59	31	12	35418	7.2	−45.6	0.5	−58.4	20.8	169.6	3.0	2.0	2.1
88	62	19	28	21	24	38355	0.9	−50.5	4.2	−58.5	370.9	60.8	3.7	2.3	2.2
88	63	19	28	36	5	38418	0.5	−51.7	0.7	−58.2	36.3	45.5	3.9	3.0	4.7
88	64	19	28	46	5	38434	1.8	−51.8	1.4	−57.8	75.3	104.3	4.5	2.0	1.5
88	65	19	28	52	6	38430	2.7	−51.9	1.0	−57.5	81.0	138.3	4.4	2.1	1.7
88	66	19	29	9	16	38368	2.7	−51.7	0.9	−57.2	76.6	132.8	3.1	2.1	1.8
88	67	19	29	24	6	38323	3.6	−51.7	0.5	−57.2	67.1	155.1	3.2	2.1	1.6
88	68	19	29	37	15	38364	4.1	−51.8	1.3	−57.3	66.0	143.4	3.5	2.1	1.8
88	69	19	29	50	9	38338	5.4	−51.9	0.6	−57.5	35.8	202.5	4.7	2.2	1.9
88	70	19	30	0	5	38342	6.3	−52.0	0.5	−57.6	22.2	222.0	3.9	2.4	1.5
88	71	19	30	8	5	38370	6.8	−52.2	0.4	−57.7	23.8	186.9	4.1	2.1	1.5
88	72	19	30	15	9	38322	7.2	−51.9	0.5	−57.9	29.7	194.7	3.7	1.9	2.0
88	73	19	30	27	12	38300	8.1	−52.0	0.6	−58.2	28.2	214.2	3.5	2.4	1.8
88	74	19	30	42	16	38293	9.0	−51.9	0.6	−58.4	27.7	210.3	4.0	3.8	1.8
88	75	19	31	11	41	38323	9.9	−51.9	0.7	−58.3	22.2	237.1	3.9		2.0
88	76	19	32	5	61	38278	12.6	−52.0	0.6	−58.1	17.2	130.5	3.6		2.1
88	77	19	32	46	21	38311	14.4	−52.2	0.5	−58.0	16.1	208.6	3.0	4.4	2.0

Table 10. Concluded

(b) JP-8 Fuel

Power setting, percent	Crossing number	Plume crossing time			Peak width, sec	Altitude, ft	Ambient temperature, °C	Temperature enhancement, °C	Ambient dewpoint, °C	Plume enhancement, ppmv	Emission indices (1×10^{15} kg)			
		Hr	Min	Sec							UF	NUF	F	NF
80	37	19	9	1	51	35028	–44.6	8.42	–50.3	435.4	2.8	2.7	2.1	1.9
80	38	19	9	41	13	35035	–44.9	0.78	–54.4	45.3	2.7	2.5	2.0	1.8
80	39	19	9	57	6	35092	–44.7	0.64	–56.0	42.2	2.5	3.1	2.0	1.6
80	40	19	10	3	4	35022	–44.5	0.16	–56.5	29.8		2.4	1.9	1.5
80	41	19	10	24	15	35055	–44.5	0.87	–58.2	55.8		2.4	1.9	1.7
80	42	19	10	38	6	35004	–44.4	0.34	–58.5	53.5	2.5	2.8	2.1	1.6
80	43	19	10	44	5	35062	–44.6	0.18	–58.7	14.8	2.6	2.3	2.0	1.6
80	44	19	11	1	10	35009	–44.5	1.05	–58.9	46.6	2.3	5.5	2.0	1.9
80	45	19	11	19	6	35064	–44.5	0.77	–58.9	42.7	2.9	2.5	2.1	1.6
80	46	19	11	30	6	35028	–44.3	0.41	–58.9	25.3	1.8	2.6	2.0	1.7
80	47	19	11	40	4	34905	–44.1	0.40	–58.8	32.6	3.0	3.9	2.1	
80	48	19	12	0	5	34899	–43.9	0.18	–58.3	27.9	2.4	2.6	1.8	1.6
80	49	19	13	33	7	35039	–44.4	0.36	–55.5	14.2	4.1	2.0	2.0	1.5
80	50	19	13	46	6	34987	–44.5	0.18	–55.2	13.3	2.6	2.2	1.6	1.4
80	51	19	14	13	7	35015	–44.7	0.31	–54.6	11.3	2.6	3.4	2.0	1.5
80	52	19	14	42	13	35001	–44.6	0.63	–53.8	27.4	7.1	3.3	2.7	1.7
80	53	19	15	9	6	34976	–44.5	0.53	–53.4	30.0	3.1	2.7	2.0	1.7
80	54	19	15	29	7	35003	–44.6	0.51	–53.4	23.4	3.4	2.7	2.0	1.9
85	55	19	17	24	34	35062	–41.1	14.82	–36.7	2143.8	2.0	2.0	1.4	1.3
85	56	19	17	51	18	35033	–43.6	2.45	–42.5	255.8	2.4	2.3	1.8	1.4
85	57	19	18	5	8	35017	–44.9	0.69	–45.9	65.1	2.4	2.7	2.0	2.1
85	58	19	18	22	21	35069	–44.0	0.95	–52.1	76.4	2.6	2.4	1.9	1.6
85	59	19	18	42	18	34985	–44.5	0.84	–55.2	67.9	2.2	2.2	2.0	1.5
85	60	19	19	9	35	34919	–44.4	0.63	–57.7	50.3	2.1	2.2	1.9	1.5

Table 11. Flight 17, New Jersey F-16

(a) High Sulfur Content Fuel

Power setting, percent	Crossing number	Plume crossing time			Peak width, sec	Altitude, ft	Plume age	Ambient temperature, °C	Temperature enhancement, °C	Ambient dewpoint, °C	Plume enhancement, ppmv	Emission indices (1×10^{15} kg)			
		Hr	Min	Sec								UF	NUF	F	NF
80	1	13	58	19	26	29964	0.5	−22.5	13.8	−36.9	890.7	2.5	2.8	1.6	1.5
80	2	13	58	43	22	29941	0.9	−28.0	6.9	−35.9	371.7	3.0	3.2	1.6	1.4
80	3	13	59	7	28	29987	1.4	−30.8	3.1	−43.1	211.0	6.2	3.6	1.9	1.8
80	4	13	59	35	21	29890	2.3	−30.9	0.5	−46.4	42.0		2.5	1.4	1.2
80	5	13	59	56	19	29893	3.4	−31.0	0.9	−48.2	47.7	17.2	2.7	1.6	1.4
80	6	14	0	15	12	29969	4.1	−31.1	0.4	−49.0	23.4	26.2	3.0	1.6	1.6
80	7	14	0	33	6	29861	4.7	−30.8	0.2	−49.5	3.7	36.2	3.1	2.1	1.3
80	8	14	0	50	5	29833	5.4	−30.8	0.2	−49.9	3.1	32.4	2.4	1.7	0.9
80	9	14	1	0	7	29914	5.9	−30.9	0.5	−50.1	13.7	29.3	3.1	1.4	1.3
80	10	14	1	7	6	29810	6.3	−30.8	0.5	−50.2	28.3	27.6	3.3	1.4	1.2
80	11	14	1	23	7	29946	6.3	−31.1	0.7	−50.3	25.0	30.5	3.1	1.5	1.4
80	12	14	1	33	5	29812	6.8	−30.8	0.3	−50.3	25.6	29.7	3.5	1.4	1.1
80	13	14	1	49	10	29812	7.2	−30.7	0.3	−50.0	28.9	34.3	3.5	1.6	1.4
88	15	14	7	35	17	30024	0.9	−23.4	7.9	−46.7	550.2	2.8	2.6	1.4	1.3
88	16	14	7	56	25	30081	1.4	−31.2	7.6	−36.0	500.0	3.7	2.6	1.4	1.4
88	17	14	8	30	35	29872	2.7	−31.1	2.9	−44.5	173.4	14.6	2.6	1.4	1.3
88	18	14	12	31	4	29905	3.6	−31.3	0.1	−46.8	12.7	24.3	2.4	0.9	0.9
88	19	14	12	40	10	29813	2.7	−28.8	1.9	−46.6	85.3	13.7	2.5	1.0	1.2
88	20	14	12	48	4	29760	1.8	−30.2	0.2	−46.5	148.8	5.9	1.8	1.0	1.2
88	21	14	13	16	37	29902	0.9	−30.8	3.7	−44.5	303.1		2.4	1.4	1.3
88	22	14	13	40	6	29832	3.2	−30.9	0.8	−44.4	70.6	15.2	1.4	1.2	0.9
88	23	14	13	56	15	29871	4.5	−31.0	0.6	−44.7	50.2	31.3	2.4	1.3	1.2
88	24	14	14	49	59	29949	5.4	−31.3	1.2	−46.0	40.6	40.6	2.5	1.4	1.3

Table 11. Concluded

(b) JP-8 Fuel

Power setting, percent	Crossing number	Plume crossing time			Peak width, sec	Altitude, ft	Ambient temperature, °C	Temperature enhancement, °C	Ambient dewpoint, °C	Plume enhancement, ppmv	Emission indices (1×10^{15} kg)			
		Hr	Min	Sec							UF	NUF	F	NF
80	26	14	21	8	67	29778	–30.7	1.32	–45.4	76.3	2.2	2.9	1.6	1.6
80	27	14	21	48	11	29772	–30.9	0.83	–45.4	37.8	2.7	2.7	1.6	1.5
80	28	14	21	57	7	29801	–30.8	0.12	–45.6	20.0	2.3	2.7	1.5	1.3
85	29	14	26	33	30	29867	–26.3	14.29	–32.0	974.0	2.0	2.1	1.4	1.3
85	30	14	27	2	26	29885	–27.4	3.95	–40.8	410.6	2.0	1.8	1.3	1.2
85	31	14	27	32	34	29852	–29.6	2.65	–47.2	102.1	2.0	2.2	1.3	1.3
85	32	14	27	56	13	29844	–31.0	1.13	–48.4	65.3	2.3	2.1	1.4	1.4
85	33	14	28	56	8	29830	–31.2	0.64	–49.2	29.7	1.9	2.2	1.2	1.1
85	34	14	29	35	10	29627	–30.6	0.42	–46.4	22.5	2.4	2.0	1.2	1.2
85	35	14	30	11	8	29852	–31.1	0.58	–44.5	15.1	2.9	1.9	1.3	1.2

Table 12. Flight 18, New Jersey F-16

(a) Medium Sulfur Content Fuel

Power setting, percent	Crossing number	Plume crossing time			Peak width, sec	Altitude, ft	Plume age	Ambient temperature, °C	Temperature enhancement, °C	Ambient dewpoint, °C	Plume enhancement, ppmv	Emission indices (1×10^{15} kg)			
		Hr	Min	Sec								UF	NUF	F	NF
80	1	17	57	25	12	35102	0.9	–44.1	6.7	–48.1	548.5	3.1	3.2	1.9	1.8
80	2	17	57	50	38	35133	0.5	–44.2	4.6	–45.9	457.9	2.9	2.9	1.8	1.7
80	3	17	58	26	33	34990	3.2	–44.8	0.9	–47.9	50.0	6.1	2.7	1.7	1.5
80	4	17	58	52	7	35088	4.5	–45.2	0.8	–47.6	36.5	8.0	2.3	1.7	1.4
80	5	17	59	9	9	34924	4.5	–44.7	0.6	–47.0	24.3	9.1	2.0	1.2	0.9
80	6	17	59	21	8	34963	4.5	–44.8	0.5	–47.1	20.7	8.4	1.5	1.1	0.9
80	7	17	59	29	6	35043	5.4	–45.0	0.5	–47.3	18.9	14.1	2.3	1.5	1.2
80	8	17	59	46	10	35043	5.4	–44.9	0.5	–47.8	16.9	12.6	2.6	1.4	1.4
80	9	18	0	1	19	34946	5.4	–44.6	0.6	–47.3	21.2	15.6	3.6	2.4	2.2
80	10	18	0	17	5	35013	6.3	–44.7	0.5	–47.3	22.5	16.0	3.0	1.8	1.4
80	11	18	0	42	5	35012	7.2	–44.6	0.4	–47.6	16.9	17.0	3.2	1.9	1.3
80	12	18	0	51	8	34961	8.1	–44.5	0.3	–47.7	22.3	18.4	2.6	1.8	1.6
80	13	18	1	3	6	35014	9.0	–44.6	0.5	–47.7	18.0	17.7	2.3	1.8	1.6
80	14	18	1	29	8	34856	9.0	–44.8	0.6	–48.5	15.6	22.5	2.4	1.6	1.4
80	15	18	2	15	6	34999	9.0	–44.8	0.2	–48.7	5.0	22.3	3.0	2.3	1.4
88	16	18	7	48	18	34937	0.9	–40.3	11.4	–40.8	820.6	2.3	2.2	1.5	1.4
88	17	18	8	2	8	34940	0.9	–40.7	7.5	–39.6	477.7	2.5	2.6	1.5	1.3
88	18	18	8	11	9	34898	0.9	–42.6	3.6	–43.9	367.2	2.4	2.2	1.4	1.2
88	19	18	8	30	26	34915	1.4	–43.3	3.5	–51.1	232.4	3.5	2.5	1.6	1.4
88	20	18	8	48	8	34854	1.8	–44.1	0.4	–52.5	92.1	10.3	3.2	1.6	1.0
88	21	18	9	2	9	34827	2.3	–44.2	1.2	–53.8	83.8	8.8	2.8	1.6	1.3
88	22	18	9	18	7	34827	2.7	–44.1	0.4	–53.3	39.0	12.3	2.6	1.8	1.5
88	23	18	9	25	7	34826	3.2	–44.3	0.8	–51.5	63.2	7.2	2.3	1.5	1.4
88	24	18	9	41	5	34778	3.6	–44.3	0.2	–46.7	25.1	13.3	1.9	1.8	
88	25	18	9	56	4	34849	4.5	–44.4	0.4	–45.1	32.1	11.7	2.5	1.6	0.9
88	26	18	10	11	7	34759	5.4	–44.3	0.3	–47.5	38.0	11.7	2.1	1.5	1.0
88	27	18	10	56	8	34731	11.7	–44.3	0.4	–54.1	21.5	21.3	2.3	1.6	1.3
88	28	18	13	53	4	35001	10.8	–44.6	0.5	–49.1	10.5		2.8	1.3	1.7
88	29	18	14	8	6	35067	5.4	–45.2	0.2	–50.3	11.1	12.9	3.0	1.6	1.6
88	30	18	14	25	7	34932	2.7	–44.7	0.3	–50.5	8.6	10.2	2.4	1.7	1.4
88	31	18	14	32	7	34906	1.8	–44.7	1.1	–49.5	77.4	5.8	2.3	1.6	1.3
88	32	18	14	40	6	35032	0.9	–44.9	1.1	–48.2	62.7	3.9		1.4	1.2

Table 12. Continued

(a) Concluded

Power setting, percent	Crossing number	Plume crossing time			Peak width, sec	Altitude, ft	Plume age	Ambient temperature, °C	Temperature enhancement, °C	Ambient dewpoint, °C	Plume enhancement, ppmv	Emission indices (1×10^{15} kg)			
		Hr	Min	Sec								UF	NUF	F	NF
88	33	18	14	46	5	34733	4.5	–44.0	0.6	–47.2	16.5	8.6		1.7	1.3
88	34	18	15	45	7	34905	5.4	–44.6	0.5	–49.0	2.6	9.3		1.7	1.8
80	86	18	52	20	13	37556	3.6	–50.3	1.8	–54.4	61.1	4.1	2.4	1.9	1.4
80	88	18	52	43	12	37552	6.3	–50.4	0.7	–54.4	37.4	7.1	3.5	1.9	1.9
80	89	18	52	58	6	37477	6.3	–50.1	0.6	–54.1	40.6	7.0	3.6	1.8	1.4
80	90	18	53	11	5	37431	8.1	–49.9	0.7	–54.1	41.1	8.9	3.3	1.9	1.3
80	91	18	53	19	6	37411	9.0	–50.0	0.8	–54.1	38.5	7.5	3.2	1.6	1.4
80	92	18	53	26	5	37493	9.0	–50.3	0.8	–54.2	43.3	8.8	3.1	1.8	1.3
80	93	18	53	32	5	37437	7.2	–50.4	0.3	–54.1	25.1	12.6	3.4	1.7	
80	94	18	53	42	6	37508	6.3	–50.5	0.4	–53.9	24.2	7.8	2.8	1.4	1.5
80	95	18	53	53	6	37491	7.2	–50.1	0.3	–53.7	22.2	12.7	3.3	1.3	
80	96	18	53	59	4	37523	8.1	–50.5	0.3	–53.6	26.5	10.4	3.0	1.5	1.6
80	97	18	54	5	5	37529	8.6	–50.5	0.4	–53.5	18.3	11.4	3.0	1.8	1.3
80	98	18	54	14	5	37576	9.0	–50.6	0.3	–53.5	17.4	12.3	3.3	1.7	1.2
80	99	18	54	24	5	37554	9.9	–50.6	0.4	–53.5	18.5	14.4	3.1	1.3	1.5
80	100	18	54	31	6	37552	10.8	–50.5	0.4	–53.5	19.4	10.8	3.8	1.5	1.6
80	101	18	54	40	7	37559	11.7	–50.4	0.4	–53.5	21.8	11.5	3.0	1.5	1.6
80	102	18	54	46	4	37601	12.2	–50.6	0.2	–53.6	14.6	16.2	2.8	1.8	1.7
80	103	18	54	59	11	37419	13.1	–500	0.4	–53.8	14.4	16.7	4.2	1.5	1.4
80	104	18	55	13	7	37573	14.0	–50.3	0.4	–54.1	16.6	18.8	3.7	1.8	1.8
80	105	18	55	21	7	37623	15.3	–50.5	0.3	–54.3	13.0	16.4	3.5	1.9	1.6
80	106	18	55	33	5	37596	16.2	–50.6	0.2	–54.6	11.5	18.2	4.6	2.3	1.5
80	107	18	55	51	18	37669	18.0	–50.9	0.4	–54.4	12.3	11.5	3.2	2.2	1.8

Table 12. Continued

(b) JP-8 Fuel

Power setting, percent	Crossing number	Plume crossing time			Peak width, sec	Altitude, ft	Ambient temperature, °C	Temperature enhancement, °C	Ambient dewpoint, °C	Plume enhancement, ppmv	Emission indices (1×10^{15} kg)			
		Hr	Min	Sec							UF	NUF	F	NF
78	35	18	18	59	32	34921	−44.0	6.04	−40.9	414.3	2.8	2.6	1.7	1.6
78	36	18	19	18	6	34905	−44.0	2.59	−42.8	162.1	2.6	2.5	1.7	1.4
78	37	18	19	40	20	34999	−41.8	4.00	−50.1	222.6	2.8	2.7	1.8	1.7
78	38	18	20	1	20	34916	−43.6	3.18	−44.6	165.3	3.0	3.1	1.7	1.3
78	39	18	20	14	5	34898	−43.8	0.68	−44.0	142.1	2.3	2.7	1.7	1.3
78	40	18	20	26	17	34898	−43.9	1.37	−46.6	111.5	2.7	2.6	1.8	1.7
78	41	18	23	14	19	34946	−43.7	4.09	−46.4	320.6	2.6	2.5	1.6	1.6
78	42	18	23	32	16	34882	−44.0	0.90	−45.8	78.5	2.4	3.0	1.9	1.6
78	43	18	23	59	11	34879	−44.3	0.68	−48.6	49.7	2.4	2.7	1.8	1.3
78	44	18	24	17	6	34915	−44.5	0.43	−50.0	22.7		2.7	1.5	1.6
78	45	18	24	49	4	34954	−44.7	0.05	−49.0	2.8		1.5	1.0	1.1
78	46	18	24	55	7	34867	−44.6	0.14	−49.0	8.5	4.0	2.4	2.0	1.4
78	47	18	26	15	5	34754	−44.6	0.07	−46.6	15.5	2.6	1.9	1.5	0.0
78	48	18	26	49	7	34967	−45.0	0.39	−47.6	3.4	2.2	2.4	2.2	1.8
78	49	18	26	59	5	34756	−44.5	0.21	−47.3	14.5	2.1	2.8	1.2	1.1
78	50	18	27	19	7	34916	−44.8	0.76	−46.8	13.3	1.5	1.9	0.6	0.7
78	51	18	27	25	5	34901	−44.8	0.09	−46.7	10.4	1.5	1.3	0.7	0.7
78	52	18	27	33	7	34793	−44.5	0.58	−46.8	27.6	3.6	3.5	2.1	1.9
78	53	18	27	43	8	34943	−44.9	0.70	−47.2	36.6	3.1	2.7	2.0	1.7
78	54	18	27	52	6	34824	−44.6	0.58	−47.8	34.9	3.7	3.2	1.9	1.6
78	55	18	28	18	7	34853	−44.6	0.71	−48.3	57.7	2.7	2.8	1.7	1.5
85	56	18	29	21	10	34917	−43.5	7.36	−47.5	538.4	2.6	2.5	1.6	1.5
85	57	18	29	36	19	34871	−44.3	2.53	−45.7	184.8	2.7	2.4	1.6	1.4
85	58	18	29	54	8	34845	−44.6	0.86	−47.3	69.7	2.2	2.2	1.6	1.2
85	59	18	30	19	6	34910	−44.9	0.67	−51.3	40.7	2.9	3.1	1.5	1.3
85	60	18	30	32	5	34893	−45.2	0.94	−52.0	33.5	1.3	1.8	1.5	1.1
85	61	18	30	41	5	34855	−45.0	0.47	−51.5	41.6	2.4	2.3	1.4	1.0
85	62	18	30	50	5	34825	−45.1	0.60	−50.6	38.4	1.5	1.7	1.4	0.9
85	63	18	31	11	4	34944	−45.1	0.14	−49.1	4.9		1.7	1.2	0.9
85	64	18	31	49	5	34868	−44.8	0.18	−51.6	12.3	2.5	2.1	1.5	
85	65	18	32	12	7	34901	−44.6	0.97	−53.5	62.3	3.6	2.4	1.6	1.3
85	66	18	32	22	5	34873	−44.5	0.60	−53.7	37.2	2.4	1.7	1.5	1.2
85	67	18	32	52	6	34811	−44.3	0.80	−50.0	67.0	2.4	2.6	1.5	1.2
85	68	18	33	43	7	34776	−44.5	0.28	−47.6	23.0	2.2	2.5	1.5	1.2

Table 12. Concluded

(b) Concluded

Power setting, percent	Crossing number	Plume crossing time			Peak width, sec	Altitude, ft	Ambient temperature, °C	Temperature enhancement, °C	Ambient dewpoint, °C	Plume enhancement, ppmv	Emission indices (1×10^{15} kg)			
		Hr	Min	Sec							UF	NUF	F	NF
85	69	18	33	59	16	34804	–44.4	0.40	–46.4	26.6	2.1	2.1	1.5	1.4
85	70	18	34	22	5	34750	–44.4	0.09	–47.5	3.9	1.8	2.6	1.8	1.5
85	71	18	35	4	24	34824	–44.5	0.43	–51.3	15.8	2.6	2.1	1.7	1.6
85	72	18	35	33	13	34637	–44.1	0.62	–50.0	11.7	2.3	2.6	1.7	1.5
85	73	18	36	9	20	34894	–45.5	1.31	–50.8	9.9	2.2	2.6	1.8	1.7
85	74	18	36	41	10	34684	–44.2	0.42	–50.9	10.3	3.4	2.4	1.4	1.5
85	75	18	44	2	5	37882	–51.6	0.13	–54.3	8.2		3.3	1.5	1.1
85	76	18	44	19	15	37841	–51.4	0.98	–53.9	28.6	3.0	2.4	1.7	1.3
85	77	18	44	41	5	37802	–51.1	0.16	–54.1	42.4	3.3	2.2	1.5	
85	78	18	44	48	4	37930	–51.2	0.85	–54.3	54.0	2.5	1.8	1.6	
85	79	18	45	6	8	37876	–51.0	0.56	–54.9	36.3	3.1	2.9	1.9	1.4
85	80	18	45	22	6	37803	–50.9	0.84	–55.2	47.8	2.6	2.9	1.5	1.5
85	81	18	45	40	10	37825	–50.7	0.81	–55.1	56.2		2.9	1.7	1.5
85	82	18	45	50	9	37854	–50.8	0.52	–54.9	35.5		1.7	0.7	

Table 13. Flight 19, New Jersey F-16

(a) Low Sulfur Content Fuel

Power setting, percent	Crossing number	Plume crossing time			Peak width, sec	Altitude, ft	Plume age	Ambient temperature, °C	Temperature enhancement, °C	Ambient dewpoint, °C	Plume enhancement, ppmv	Emission indices (1×10^{15} kg)			
		Hr	Min	Sec								UF	NUF	F	NF
80	3	13	55	7	39	35083	0.9	–45.7	1.6	–47.6	106.2	2.9	2.8	1.9	1.9
80	4	13	57	38	27	34866	7.2	–45.6	0.7	–49.4	31.3	3.7	3.1	1.9	1.9
80	6	14	4	26	12	34511	15.3	–44.7	0.4	–48.5	12.8	3.9	3.0	1.8	1.7
80	7	14	8	40	20	34869	1.8	–45.6	2.6	–49.0	411.9	2.8	3.0	1.8	1.7
80	8	14	9	4	28	34753	2.7	–45.6	1.4	–47.6	91.7			1.4	1.4
80	9	14	10	2	10	34732	3.6	–45.6	0.7	–48.8	51.4	2.2		1.9	1.5
80	10	14	10	13	7	34785	3.6	–45.8	0.8	–48.4	38.9	3.0	3.3	1.8	1.5
80	11	14	10	57	8	34832	6.3	–45.6	0.5	–46.9	27.7	2.9	2.8	1.5	1.6
88	14	14	14	54	31	34845	0.9	–45.6	4.4	–44.5	314.8		2.8	1.8	1.7
88	15	14	15	25	15	34830	1.8	–46.0	1.2	–46.1	75.2	3.6	2.6	1.7	1.5
88	16	14	15	36	6	34842	2.7	–45.8	0.3	–46.9	34.7	2.6	2.6	1.7	1.3
88	17	14	15	51	17	34795	3.2	–45.7	0.9	–48.9	60.4	3.0	3.2	1.7	1.4
88	18	14	16	7	9	34849	4.5	–45.7	1.0	–49.6	54.3	3.0	2.7	1.7	1.5
88	19	14	16	19	4	34891	6.3	–45.8	0.3	–49.8	19.1	6.1	2.5	2.1	1.1
88	21	14	16	44	4	34808	8.1	–45.7	0.3	–49.0	15.9	5.2		2.0	1.4
88	22	14	19	17	5	34947	6.3	–46.2	0.4	–49.1	21.7	2.1	1.1	1.3	1.2
88	23	14	19	31	6	34884	4.5	–46.0	0.3	–49.1	27.2	3.4	3.9	2.2	2.0
88	24	14	20	26	13	34795	1.8	–45.8	0.7	–48.6	56.7	2.7	2.8	1.7	1.6
88	25	14	21	33	20	34911	0.9	–45.1	5.6	–45.8	450.3	2.4	2.8	1.5	1.6
88	26	14	21	51	16	34790	1.4	–45.5	1.0	–44.5	71.1	2.6	3.2	1.6	1.4
88	27	14	22	13	7	34721	2.7	–45.5	0.8	–45.7	67.4	1.9	2.8	1.5	1.3
88	28	14	22	27	7	34606	3.6	–45.4	1.1	–47.3	65.2	3.7	4.2	1.7	1.4
88	29	14	23	8	7	34557	5.0	–45.4	0.5	–51.5	31.7	3.0	2.8	1.6	1.5
88	30	14	23	27	8	34866	5.4	–45.9	0.7	–52.8	32.1	4.1	2.5	1.7	1.5
88	31	14	23	36	7	34732	6.3	–45.7	0.5	–53.2	34.1	2.7	2.6	1.6	1.4

Table 13. Concluded

(b) JP-8 Fuel

Power setting, percent	Crossing number	Plume crossing time			Peak width, sec	Altitude, ft	Ambient temperature, °C	Temperature enhancement, °C	Ambient dewpoint, °C	Plume enhancement, ppmv	Emission indices (1×10^{15} kg)			
		Hr	Min	Sec							UF	NUF	F	NF
80	33	14	30	5	18	34881	–45.7	1.07	–46.3	66.7	2.8	2.6	2.0	1.7
80	34	14	30	37	12	34926	–46.1	0.71	–47.5	40.7	2.1	2.2	1.8	1.6
80	35	14	30	54	11	34956	–46.1	0.60	–48.3	31.8	2.4	2.5	1.7	1.3
80	36	14	31	3	7	34967	–46.2	0.28	–48.5	11.6	2.9	2.3	2.0	1.4
80	37	14	31	13	6	34830	–46.0	0.44	–48.5	21.0	2.9	3.0	2.3	1.9
80	38	14	31	22	8	35039	–46.4	0.66	–48.3	23.9	2.8	3.2	2.3	1.9
80	39	14	31	31	6	34902	–46.1	0.42	–48.1	20.1	3.8	2.9	2.2	1.7
80	40	14	31	48	5	34948	–46.3	0.42	–47.5	18.0	3.7	3.0	2.2	1.6
80	41	14	31	57	4	34817	–46.2	0.24	–47.3	13.5	2.7	2.2	1.9	0.0
80	42	14	32	7	4	34808	–46.2	0.32	–47.0	4.0	3.9	6.9	1.4	1.3
80	43	14	32	17	5	34785	–46.0	0.20	–47.0	14.1	2.6	2.0	2.0	1.3
80	44	14	32	30	10	34812	–45.9	0.40	–47.3	14.1	2.9	1.9	2.0	1.5
85	45	14	39	33	7	35004	–46.8	2.61	–51.5	265.8	2.3	2.1	1.8	1.3
85	46	14	39	52	9	35059	–46.9	0.49	–51.7	9.4			2.0	
85	47	14	41	12	14	34848	–45.8	1.49	–52.7	491.8	2.4	2.3	1.7	1.4
85	48	14	41	26	5	34911	–46.0	0.13	–52.7	16.6	2.1	2.3	2.1	1.3
85	49	14	41	33	9	34824	–45.8	2.16	–52.6	250.8	2.3	2.3	1.8	1.3
85	50	14	41	53	26	34895	–45.7	2.98	–51.0	222.5	2.5	2.5	1.9	1.6
85	51	14	42	11	5	34988	–46.0	0.51	–50.9	36.2	2.6	2.4	1.8	1.0
85	52	14	42	20	11	34905	–46.0	0.61	–51.3	45.1	2.7	2.6	1.8	1.7
85	53	14	42	29	6	34924	–45.8	0.94	–51.7	60.7	2.3	1.9	1.7	1.2
85	54	14	42	41	7	34961	–45.9	0.99	–52.6	61.6	2.2	2.0	1.8	1.4
85	55	14	42	54	16	34853	–45.8	0.46	–54.0	46.2	2.2	2.2	1.7	1.3
85	56	14	43	11	8	34963	–46.0	0.82	–54.9	45.3	2.6	2.2	1.8	1.6
85	57	14	43	24	6	34931	–46.1	0.50	–55.5	25.5	2.4	2.9	1.7	1.3
85	58	14	43	45	8	34944	–46.2	0.17	–56.4	3.0		2.3	1.5	1.2
85	59	14	45	52	5	34739	–45.6	0.49	–48.0	37.2	4.6	3.9	1.8	1.3
85	60	14	46	14	5	35086	–46.1	0.95	–46.6	56.7	2.1	2.4	1.8	1.1
85	61	14	46	26	5	35014	–46.0	1.10	–47.2	47.7	3.9	6.3	1.7	1.3
85	62	14	46	35	6	34954	–45.8	0.96	–47.9	64.1	2.4	2.3	1.7	1.3
85	63	14	46	43	6	34956	–45.9	0.96	–48.6	59.3	2.0	2.1	1.7	1.1
85	64	14	46	52	5	34826	–45.7	0.95	–49.2	60.2	3.4	3.0	1.9	1.4
85	65	14	47	32	6	34863	–46.0	0.39	–51.5	22.3	1.8	1.9	1.7	1.3
85	66	14	47	59	6	34955	–46.0	0.28	–53.1	13.8	2.6	1.8	1.6	1.3
85	67	14	48	33	10	34842	–46.6	0.68	–54.9	17.1	2.3	2.7	1.7	1.6

Table 14. Flight 20, New Jersey F-16

(a) Low Sulfur Content Fuel

Power setting, percent	Crossing number	Plume crossing time			Peak width, sec	Altitude, ft	Plume age	Ambient temperature, °C	Temperature enhancement, °C	Ambient dewpoint, °C	Plume enhancement, ppmv	Emission indices (1×10^{15} kg)			
		Hr	Min	Sec								UF	NUF	F	NF
80	3	18	0	53	15	29941	0.9	–30.5	2.1	–50.5	270.7	3.3	2.6	1.9	1.2
80	4	18	1	8	12	29958	1.8	–32.4	1.6	–50.5	128.6	2.7	2.2	1.6	1.0
80	5	18	1	22	15	29889	2.7	–32.8	1.0	–50.6	58.7	3.4	2.7	1.6	1.1
80	6	18	1	36	11	29894	3.2	–33.0	1.1	–50.8	48.8	3.3	2.8	1.5	1.0
80	7	18	1	49	6	29930	3.6	–33.2	0.5	–51.1	23.8	2.5	2.1	1.3	0.8
80	8	18	1	59	6	29947	4.1	–33.3	0.4	–51.3	26.3	2.8	2.1	1.3	0.9
80	9	18	2	7	6	29883	4.5	–33.1	0.3	–51.4	20.8	2.4	2.9	1.2	1.0
80	10	18	2	27	21	29881	5.4	–33.1	0.5	–51.6	31.3	3.0	2.3	1.7	1.2
80	11	18	2	45	6	29919	5.9	–33.2	0.5	–51.7	25.2	3.0	2.7	1.6	1.1
80	12	18	2	58	5	29928	6.3	–33.2	0.2	–51.8	5.4		1.8	1.4	0.9
80	13	18	3	51	12	29752	8.1	–32.9	0.6	–52.2	21.1	3.0	2.5	1.6	1.1
80	14	18	7	11	27	29901	0.9	–32.5	5.2	–52.9	403.9	3.1	2.5	1.7	1.2
80	15	18	7	35	11	29887	2.7	–32.7	0.8	–53.1	66.0	2.9	2.5	1.6	1.2
80	16	18	8	4	7	29837	5.4	–32.6	0.4	–53.5	32.4	3.1	2.4	1.6	1.3
80	17	18	8	49	8	29712	11.7	–32.6	0.3	–53.9	16.7	2.5	2.4	1.7	1.2
80	18	18	9	13	7	29785	13.5	–32.9	0.4	–54.1	15.3	2.2	2.6	1.5	1.2
88	20	18	15	6	20	30027	0.9	–32.0	6.9	–38.9	396.5	2.6	2.1	1.6	1.2
88	21	18	15	32	31	30003	1.8	–33.4	3.1	–47.7	192.0	2.7	2.1	1.5	1.2
88	22	18	15	55	6	29994	2.7	–33.3	0.9	–49.4	60.0	2.4	2.4	1.2	1.2
88	23	18	16	2	7	30047	2.7	–33.5	1.2	–50.5	56.5	2.4	2.1	1.4	1.2
88	24	18	16	14	7	29974	3.6	–33.4	0.9	–51.7	74.2	2.7	2.6	1.3	1.1
88	25	18	16	33	7	29940	3.6	–33.5	0.7	–53.1	56.0	2.4	1.8	1.3	1.1
88	26	18	17	8	8	29893	4.5	–33.1	0.5	–54.6	48.2	2.9	2.3	1.4	1.2
88	27	18	19	17	4	29949	8.1	–33.3	0.4	–55.7	22.1	1.6	2.0	0.9	1.4
88	28	18	22	4	19	29965	0.9	–26.7	7.5	–52.3	811.5	2.3	1.7	1.4	1.1
88	29	18	22	21	15	29955	1.4	–32.2	3.3	–42.1	342.9	2.6	2.1	1.7	1.3
88	30	18	22	46	32	29964	2.7	–33.3	2.1	–49.8	98.4	2.4		1.1	1.2
88	31	18	23	12	7	30023	5.0	–33.8	0.3	–51.7	4.0			1.1	1.2
88	32	18	24	14	5	29864	6.3	–33.2	0.7	–55.4	39.3	2.2	1.8	1.1	1.4
88	33	18	24	28	5	29933	5.4	–33.0	0.8	–55.6	44.5	1.8	1.5	1.2	1.5
88	34	18	24	40	6	30049	5.4	–33.2	0.7	–55.9	35.2	3.0	2.1	1.4	1.6
88	35	18	24	55	5	29947	5.9	–32.9	0.5	–56.0	33.3	2.2	1.4	1.1	1.3

Table 14. Concluded

(b) JP-8 Fuel

Power setting, percent	Crossing number	Plume crossing time			Peak width, sec	Altitude, ft	Ambient temperature, °C	Temperature enhancement, °C	Ambient dewpoint, °C	Plume enhancement, ppmv	Emission indices (1×10^{15} kg)			
		Hr	Min	Sec							UF	NUF	F	NF
88	50	18	41	17	13	29775	–32.5	4.64	–55.2	254.3	2.2	2.4	1.7	1.7
88	51	18	41	39	22	29716	–32.3	1.27	–54.5	75.4	2.3	2.7	1.7	1.5
88	52	18	42	1	19	29705	–32.2	1.05	–54.3	71.8	2.3	2.5	1.7	1.7
88	53	18	42	21	11	29695	–32.4	1.01	–54.4	65.2	2.8	2.5	1.6	1.6
88	54	18	42	38	18	29769	–32.1	0.71	–54.4	49.0	2.3	2.5	1.6	1.7
88	55	18	42	54	12	29781	–32.9	0.80	–54.4	34.6	2.2	2.3	1.7	1.8
88	56	18	43	20	12	29603	–32.6	0.64	–54.5	35.0	2.3	2.2	1.7	1.6
88	57	18	44	27	6	29743	–33.0	0.27	–54.9	16.2	2.1	2.7	1.7	1.4
88	58	18	44	51	7	29636	–32.8	0.39	–55.2	11.4	2.1	1.7	1.5	1.5

Table 15. Summary of F-16 Observations

Flight number	Source aircraft	Aircraft fuel	Power setting, percent	Altitude, ft	Ambient temperature, °C	Dewpoint, °C	Number of points	Total UF EI (1×10^{15}/kg)			Nonvolatile UF EI (1×10^{15}/kg)			Total F EI (1×10^{15}/kg)			Nonvolatile F EI (1×10^{15}/kg)		
								Avg	Med	Std	Avg	Med	Std	Avg	Med	Std	Avg	Med	Std
5	NJANG-1	JP-8	70	25737	–26.3	–31.2	10	22.6	6.1	31.2	5.1	5.2	1.4	2.1	2.4	0.8	1.9	2.3	0.8
5	NJANG-1	JP-8	78	29716	–36.4	–40.0	16	5.8	5.8	0.5	5.6	5.7	0.7	2.2	2.3	0.2	2.1	2.2	0.2
5	NJANG-1	JP-8	83	25273	–24.6	–30.6	13	5.7	5.8	0.5	5.4	5.4	0.4	2.4	2.5	0.2	1.9	2.0	0.3
5	NJANG-1	JP-8	90	23928	–21.7	–26.5	15	4.8	4.8	0.7	4.0	3.9	0.7	1.9	1.9	0.2	1.6	1.5	0.2
6	VANG-1	JP-8+100	78	29867	–39.8	–51.8	3	6.1	6.4	0.6	4.3	4.4	0.6	1.8	1.8	0.1	1.6	1.7	0.4
6	VANG-1	JP-8+100	78	34968	–50.8	–55.9	11	44.6	34.4	30.2	3.9	3.8	0.7	2.2	2.3	0.2	1.7	1.8	0.4
6	VANG-2	JP-8+100	78	29875	–40.0	–52.0	13	7.5	6.9	1.6	5.1	4.8	0.8	2.3	2.3	0.2	2.4	2.5	0.2
6	VANG-2	JP-8+100	78	34752	–50.8	–54.8	10	16.5	8.1	21.8	4.7	5.1	1.3	2.6	2.8	0.6	2.3	2.5	0.6
6	VANG-3	JP-8+100	78	29912	–40.0	–49.0	12	142.9	62.1	187.2	7.9	6.1	5.4	10.6	2.7	18.4	2.6	2.6	0.5
6	VANG-3	JP-8+100	78	34813	–50.6	–54.0	10	20.2	11.1	14.9	5.3	5.4	1.0	3.1	3.0	0.5	2.8	2.9	0.4
6	VANG-1	JP-8+100	85	34353	–50.0	–54.7	5	11.1	11.2	3.7	4.6	4.7	0.9	2.2	2.2	0.2	2.1	2.2	0.2
6	VANG-1	JP-8+100	88	30016	–40.6	49.9	9	9.3	9.3	1.4	3.7	3.8	0.3	1.8	1.8	0.1	1.8	1.8	0.1
6	VANG-2	JP-8+100	88	29913	–40.2	–48.0	9	8.2	8.6	1.1	4.5	4.6	0.6	2.2	2.2	0.2	2.1	2.0	0.2
6	VANG-3	JP-8+100	88	29852	–40.0	–48.0	8	51.2	33.8	48.1	5.5	5.2	1.1	2.5	2.5	0.4	2.4	2.3	0.3
6	VANG-3	JP-8+100	90	34742	–50.8	–53.8	13	21.3	12.3	17.1	5.1	4.8	0.9	3.1	3.1	0.2	2.7	2.7	0.2
6	VANG-3	JP-8+100	100	34883	–51.2	–54.5	9	634.9	630.0	135.9	74.9	76.0	37.0	258.3	251.0	100.5	2.6	1.9	1.4
7	VANG-4	JP-8+100	78	29528	–38.1	–42.1	6	16.3	15.3	5.2	3.8	3.8	0.5	1.6	1.6	0.2	1.7	1.6	0.2
7	VANG-4	JP-8+100	78	34592	–49.7	–53.2	1	4.7	4.7	0.0	4.0	4.0	0.0	2.1	2.1	0.0	2.1	2.1	0.0
7	VANG-5	JP-8+100	78	29950	–39.4	–41.1	8	6.5	6.3	1.6	4.8	4.7	0.9	2.5	2.5	0.5	2.5	2.3	0.5
7	VANG-4	JP-8+100	88	29556	–38.3	–42.7	2	62.9	62.9	0.0	3.8	3.8	0.5	0.8	0.8	1.1	1.5	1.5	0.1
7	VANG-5	JP-8+100	88	29798	–39.0	–42.5	7	23.6	16.3	14.1	4.9	4.9	0.6	2.5	2.5	0.2	2.4	2.2	0.2
10	NJANG-2	JP-8	78	27704	–29.0	–39.3	2	2.4	2.4	0.7	2.6	2.6	0.5	1.7	1.7	0.6	1.4	1.4	0.4
10	NJANG-2	JP-8	83	29386	–32.5	–40.6	11	2.8	2.9	0.3	2.9	3.0	0.3	2.0	2.1	0.2	1.5	1.5	0.2
10	NJANG-2	JP-8	85	38645	–58.0	–59.4	23	129.6	4.3	178.2	11.5	3.6	11.9	48.6	2.8	78.1	2.4	1.7	2.2
10	NJANG-2	JP-8	90	29270	–32.5	–41.7	7	2.7	2.7	0.3	2.4	2.3	0.2	1.6	1.7	0.1	1.3	1.3	0.1
14	NJANG-3	High S	80	30462	–33.2	–45.8	13	96.8	87.2	58.3	3.6	3.7	0.5	1.5	1.5	0.2	1.4	1.4	0.1
14	NJANG-4	JP-8	80	30398	–33.1	–46.4	5	2.3	2.1	0.5	2.1	2.1	0.3	1.3	1.3	0.1	1.3	1.2	0.1
14	NJANG-4	JP-8	88	30426	–33.0	–45.8	11	2.2	2.1	0.3	2.0	1.9	0.2	1.3	1.3	0.1	1.3	1.3	0.1

Table 15. Concluded

Flight number	Source aircraft	Aircraft fuel	Power setting, percent	Altitude, ft	Ambient temperature, °C	Dewpoint, °C	Number of points	Total UF EI (1×10^{15}/kg)			Nonvolatile UF EI (1×10^{15}/kg)			Total F EI (1×10^{15}/kg)			Nonvolatile F EI (1×10^{15}/kg)		
								Avg	Med	Std	Avg	Med	Std	Avg	Med	Std	Avg	Med	Std
15	NJANG-3	High S	80	35334	–45.4	–53.9	20	99.9	96.8	46.2	2.6	2.6	0.4	2.0	1.9	0.4	1.5	1.5	0.2
15	NJANG-3	High S	80	38348	–51.8	–57.8	14	161.7	171.0	57.6	3.8	3.8	0.5	2.5	2.2	0.7	2.0	1.8	0.8
15	NJANG-4	JP-8	80	35012	–44.5	–56.2	18	3.0	2.6	1.2	2.9	2.6	0.8	2.0	2.0	0.2	1.6	1.6	0.2
15	NJANG-3	High S	85	35360	–45.1	–55.6	15	89.6	83.7	48.8	3.0	2.9	0.4	2.0	2.0	0.2	1.7	1.6	0.2
15	NJANG-4	JP-8	88	35014	–43.8	–48.4	6	2.3	2.3	0.2	2.3	2.2	0.2	1.8	1.9	0.2	1.6	1.5	0.3
17	NJANG-3	Med S	80	29895	–30.0	–46.9	13	22.9	28.5	12.4	3.1	3.1	0.4	1.6	1.6	0.2	1.3	1.4	0.2
17	NJANG-4	JP-8	80	29784	–30.8	–45.5	3	2.4	2.3	0.2	2.8	2.7	0.1	1.5	1.6	0.1	1.5	1.5	0.1
17	NJANG-4	JP-8	88	29822	–29.6	–44.1	7	2.2	2.0	0.3	2.0	2.1	0.2	1.3	1.3	0.1	1.2	1.2	0.1
17	NJANG-3	Med S	90	29901	–30.0	–44.7	10	16.9	14.6	12.9	2.3	2.5	0.4	1.2	1.3	0.2	1.2	1.3	0.2
18	NJANG-3	Med S	80	35006	–44.7	–47.6	15	12.9	14.1	6.4	2.6	2.6	0.5	1.7	1.8	0.3	1.4	1.4	0.3
18	NJANG-3	Med S	80	37530	–50.4	–53.9	21	11.7	11.5	4.0	3.3	3.3	0.5	1.7	1.8	0.3	1.5	1.5	0.2
18	NJANG-4	JP-8	80	34890	–44.2	–46.8	21	2.7	2.6	0.7	2.6	2.7	0.5	1.6	1.7	0.4	1.4	1.5	0.4
18	NJANG-3	Med S	88	34880	–43.9	–48.6	19	8.8	9.1	4.9	2.5	2.5	0.3	1.6	1.6	0.1	1.3	1.3	0.2
18	NJANG-4	JP-8	88	34836	–44.6	–49.9	19	2.4	2.4	0.6	2.3	2.4	0.4	1.5	1.5	0.1	1.3	1.3	0.3
18	NJANG-4	JP-8	88	37852	–51.1	–54.6	8	2.9	3.0	0.3	2.5	2.6	0.6	1.5	1.6	0.3	1.4	1.4	0.2
19	NJANG-3	Low S	80	34804	–45.5	–48.3	8	3.1	2.9	0.6	3.0	3.0	0.2	1.7	1.8	0.2	1.7	1.6	0.2
19	NJANG-4	JP-8	80	34889	–46.1	–47.6	12	3.0	2.9	0.5	2.9	2.6	1.3	2.0	2.0	0.3	1.4	1.5	0.5
19	NJANG-3	Low S	88	34804	–45.7	–48.4	17	3.3	3.0	1.1	2.8	2.8	0.7	1.7	1.7	0.2	1.5	1.4	0.2
19	NJANG-4	JP-8	88	34924	–46.0	–51.6	23	2.6	2.4	0.7	2.6	2.3	1.0	1.8	1.8	0.1	1.3	1.3	0.2
20	NJANG-3	Low S	80	29878	–32.8	–51.9	16	2.9	3.0	0.3	2.4	2.5	0.3	1.5	1.6	0.2	1.1	1.1	0.1
20	NJANG-3	Low S	88	29970	–32.7	–51.3	16	2.4	2.4	0.4	2.0	2.1	0.3	1.3	1.3	0.2	1.3	1.2	0.2
20	NJANG-4	JP-8	88	29714	–32.5	–54.6	9	2.3	2.3	0.2	2.4	2.5	0.3	1.6	1.7	0.1	1.6	1.6	0.1

Figure 1. Photograph of the Wallops Flight Facility T-39 aircraft with attached underwing aerosol probes and cabin-top aerosol and trace gas inlets.

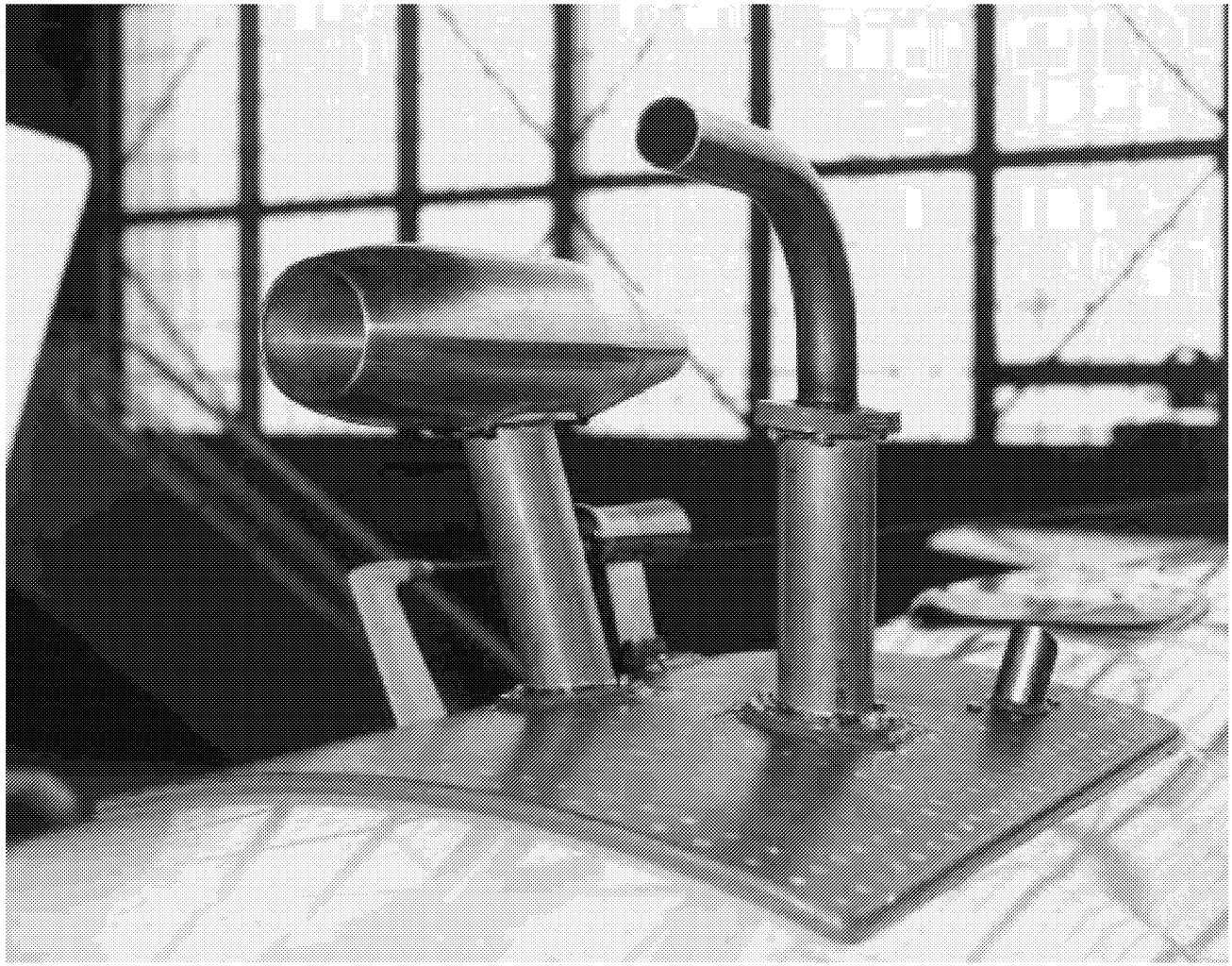

Figure 2. Photograph showing the shrouded inlet (left) and ram air inlet (right) used to sample aerosols and trace gases, respectively, aboard the T-39.

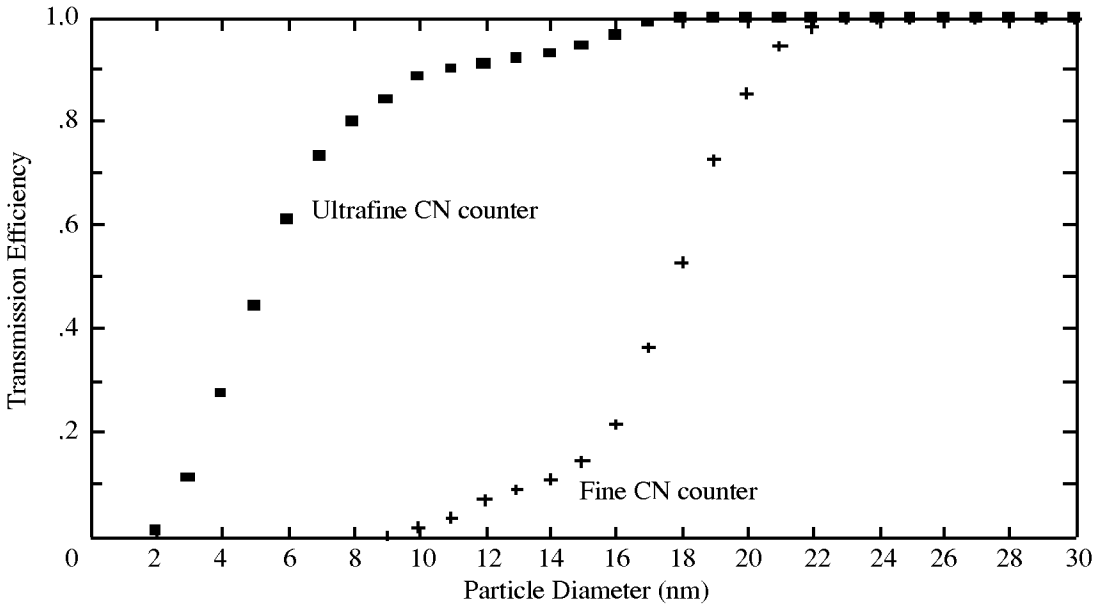

Figure 3. Response curves for the ultrafine and fine CN counters under simulated flight conditions (160 Torr pressure).

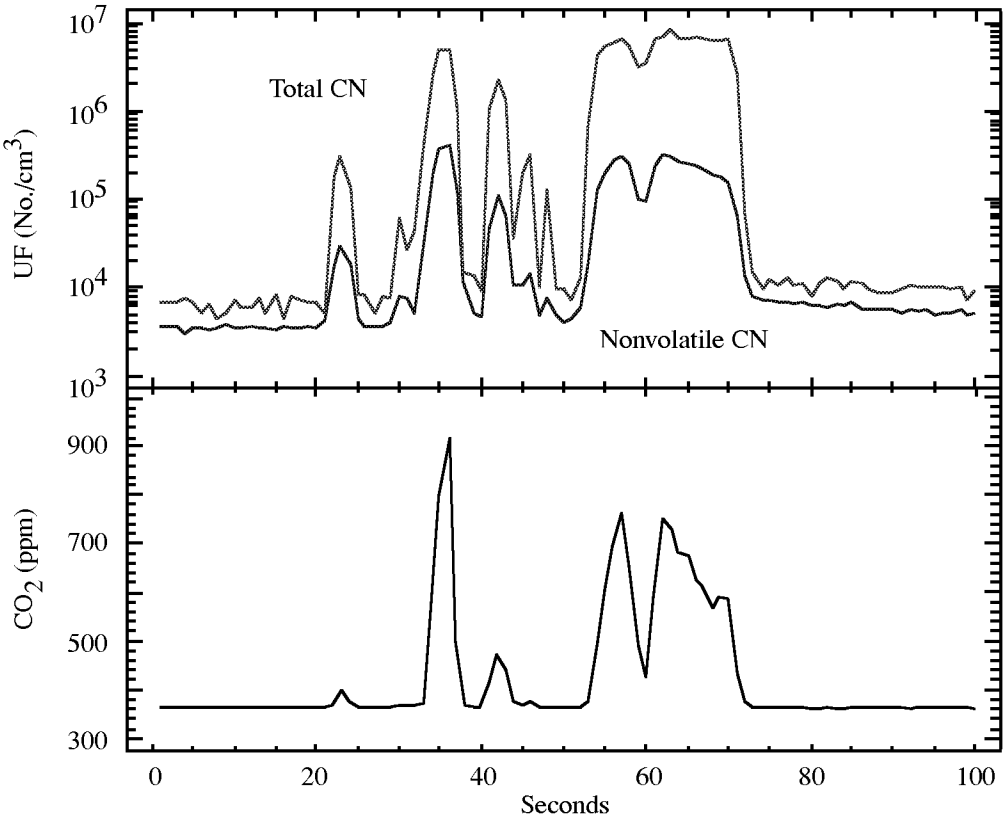

Figure 4. Example time series of aerosol and carbon dioxide concentration fluctuations during near-field aircraft plume sampling.

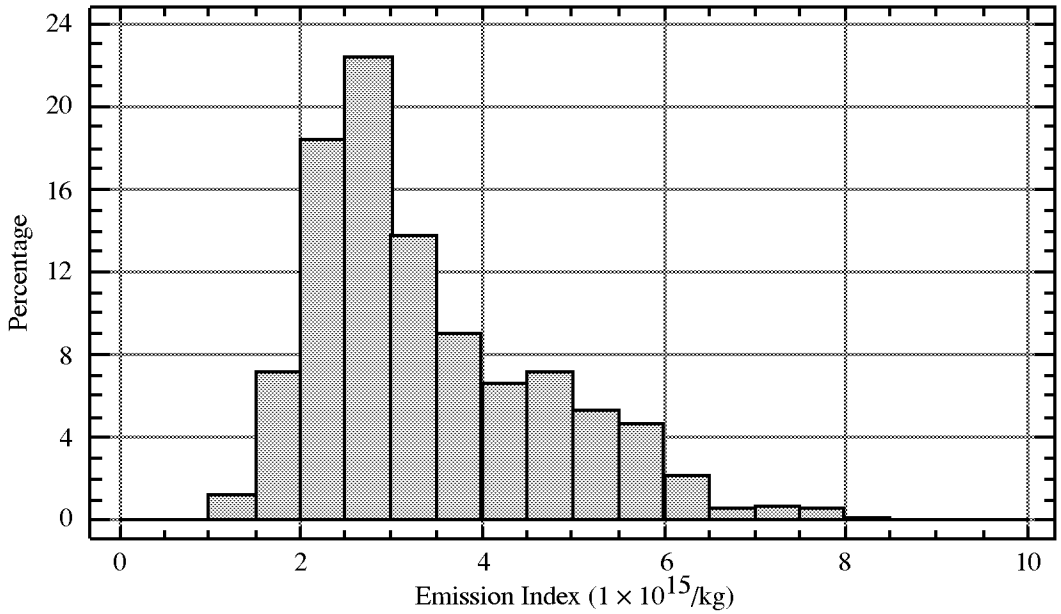

Figure 5(a). Histogram of all UF EI's recorded during the SNIF-III mission, excluding cases where afterburners were used.

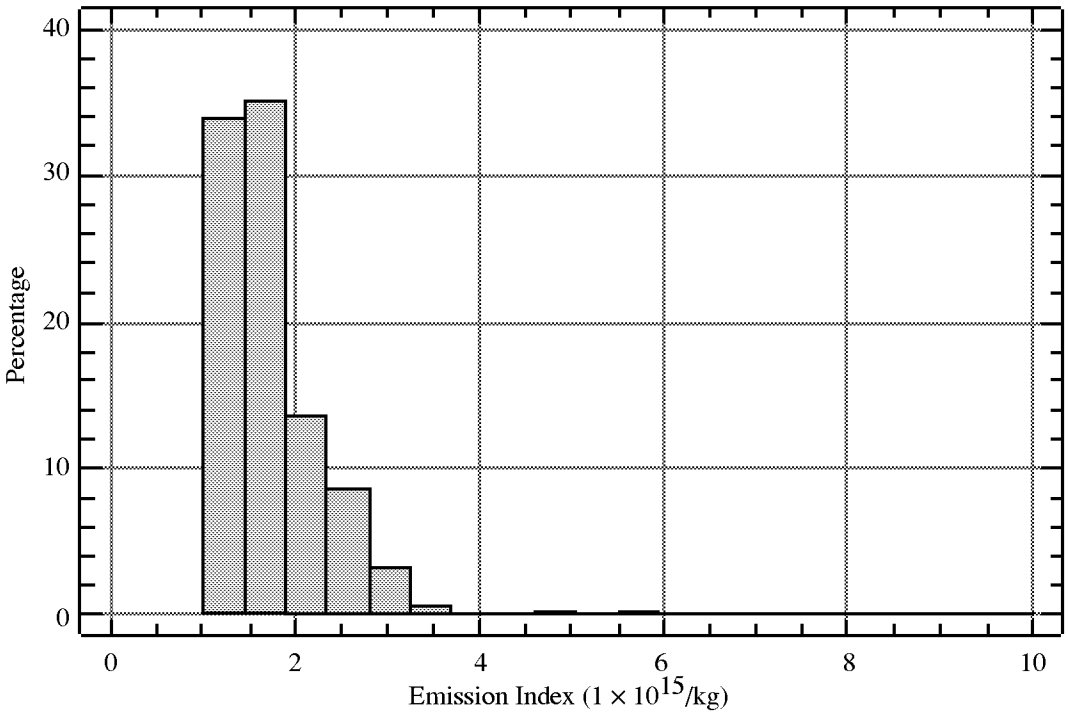

Figure 5(b). Histogram of all NF aerosol EI's recorded during SNIF-III.

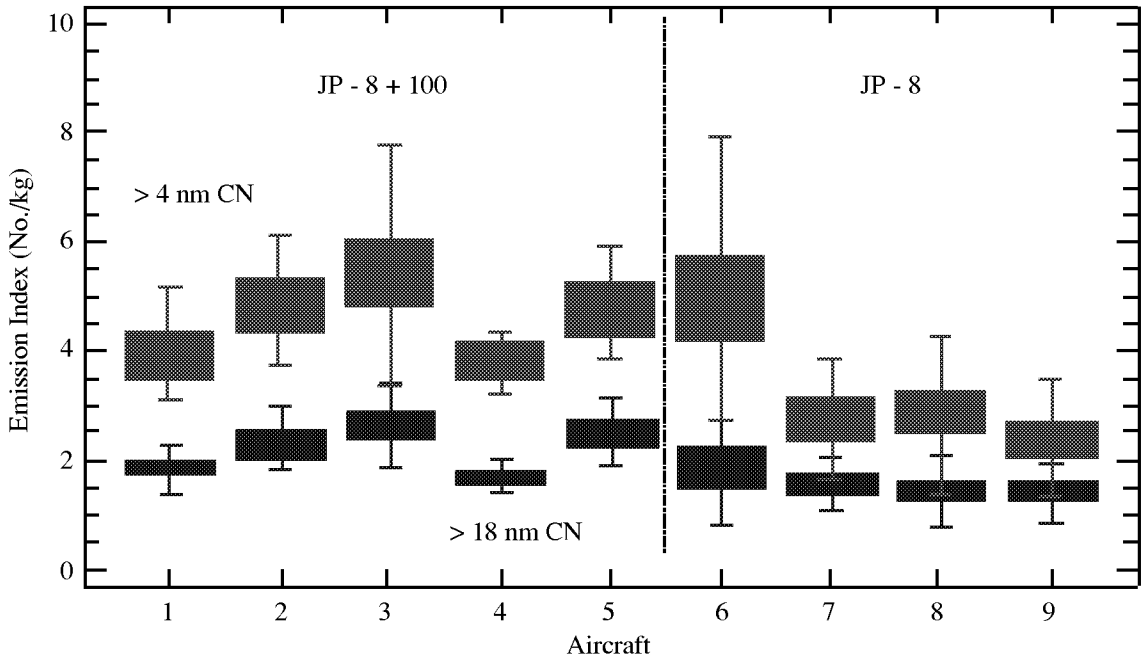

Figure 6. NUF and NF EI's for the F-16 aircraft sampled during SNIF-III. The first five aircraft were operated by VANG whereas 6 through 9 were NJANG aircraft.

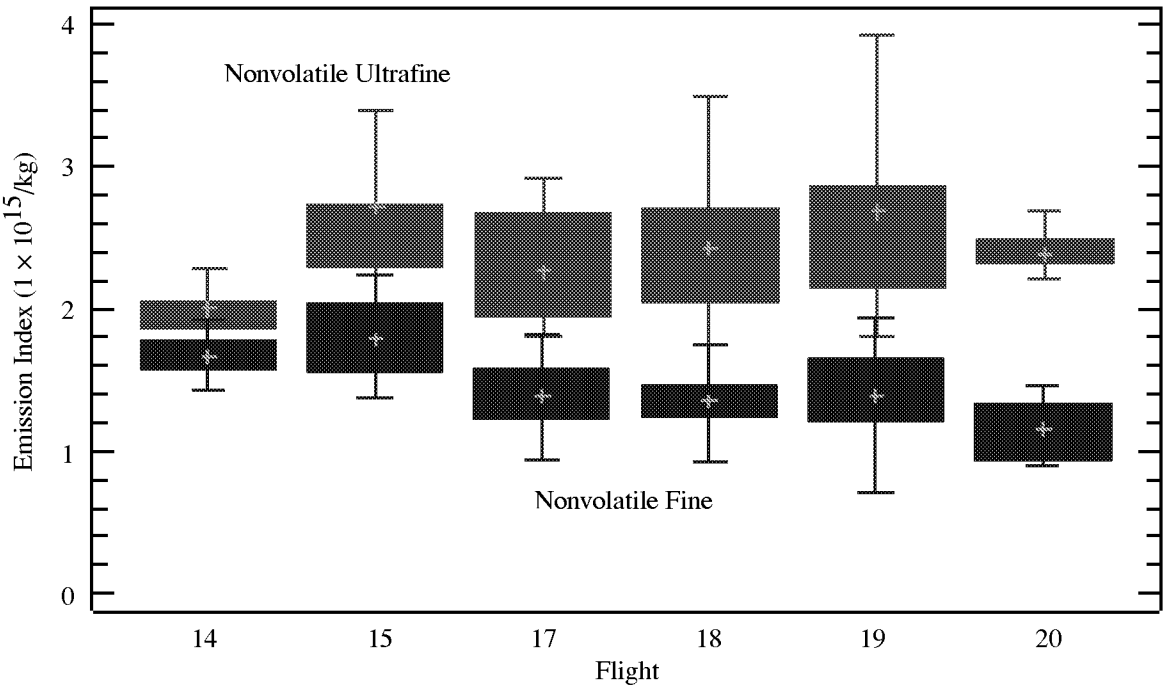

Figure 7. Nonvolatile aerosol emissions from the F-16 which burned standard JP-8 fuel during the first six S flights. In these box and whisker plots, the boxes enclose the two inner-quartiles of data while the lines extend from the 5th to 95th percentiles of the data.

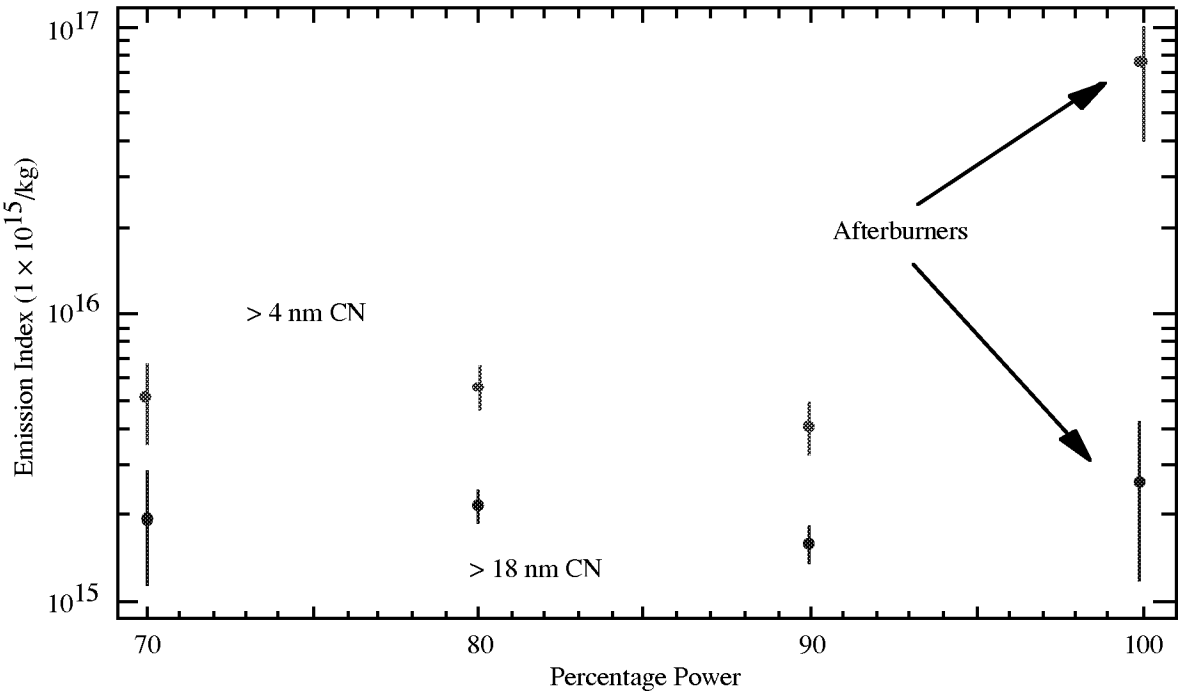

Figure 8. Nonvolatile aerosol emissions as a function of engine power setting as recorded on flight 6.

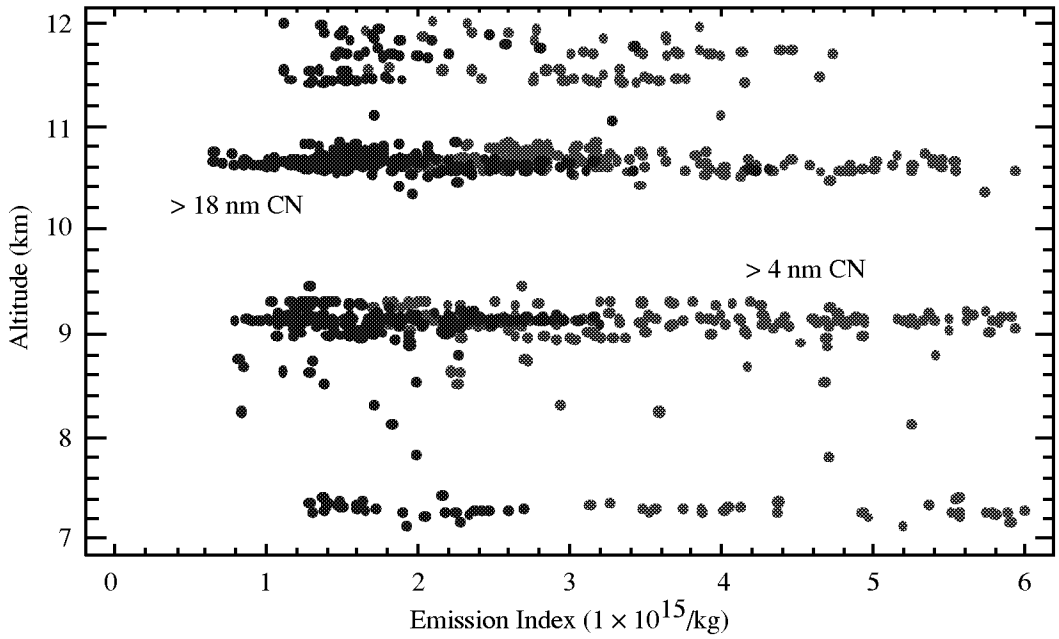

Figure 9. F-16 nonvolatile emissions plotted as a function of flight altitude.

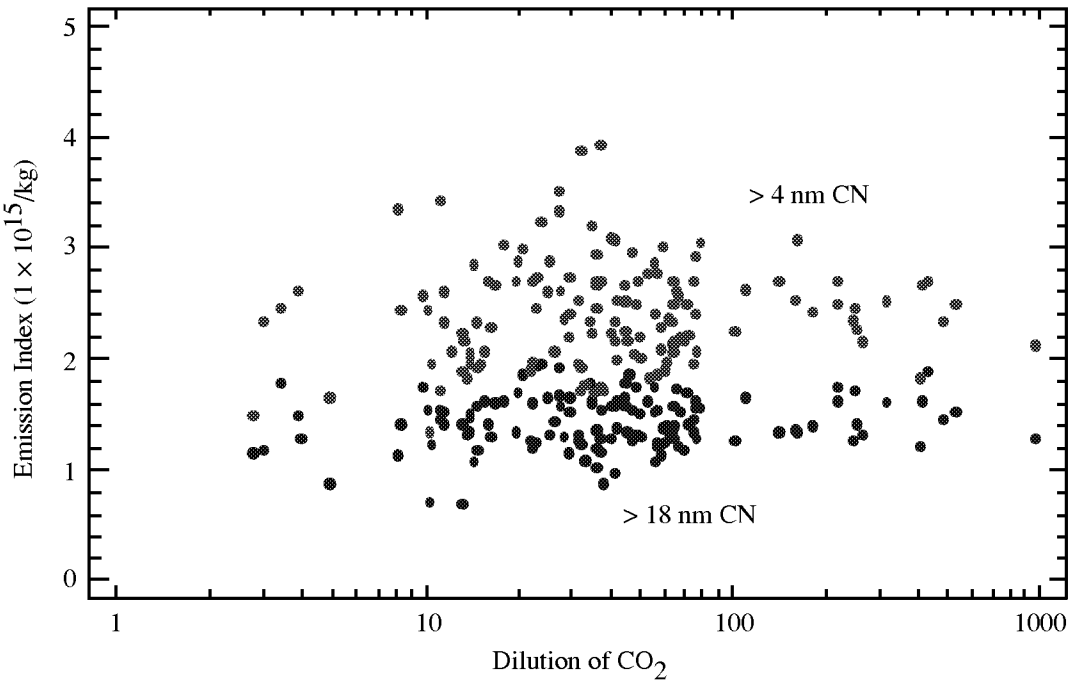

Figure 10. Nonvolatile aerosol emissions as a function of plume dilution as represented by the peak enhancement of CO_2 observed within the plume.

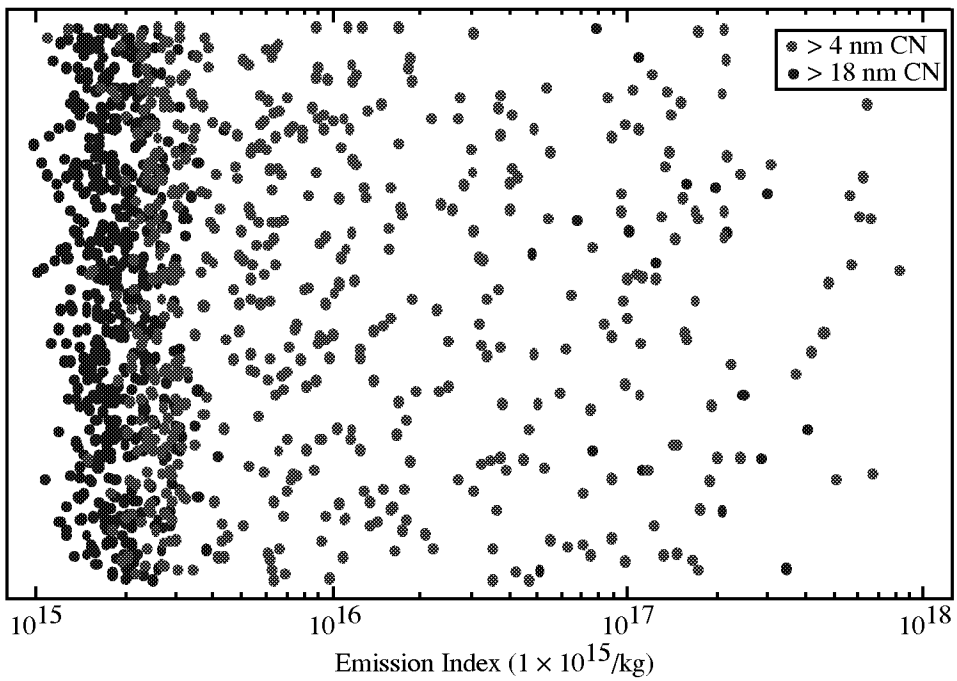

Figure 11. Randomized distribution of total aerosol emissions for all F-16 plume crossings.

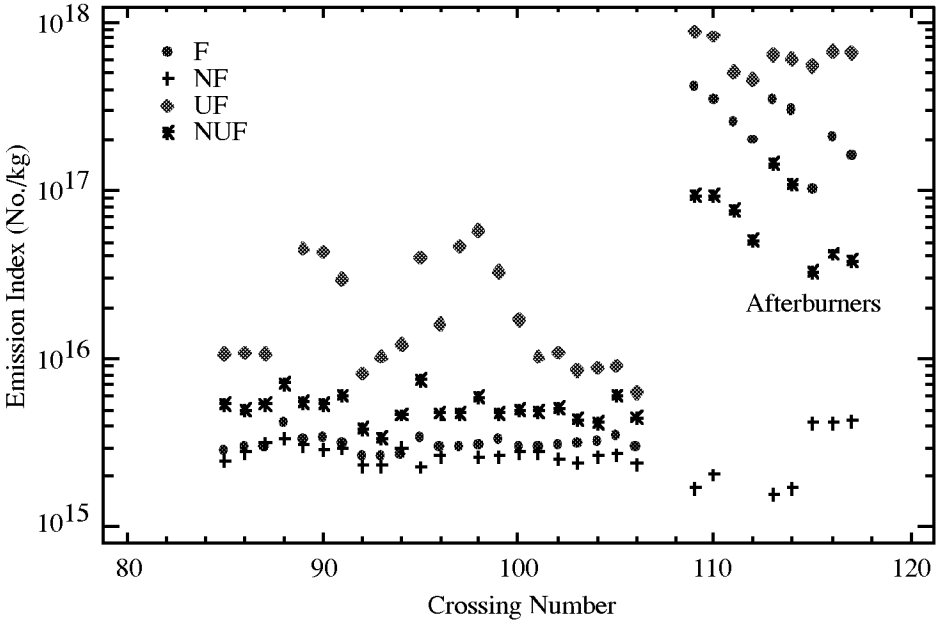

Figure 12. Plume crossings recorded during flight 6 showing the dramatic impact of afterburner ignition upon the aircraft aerosol production.

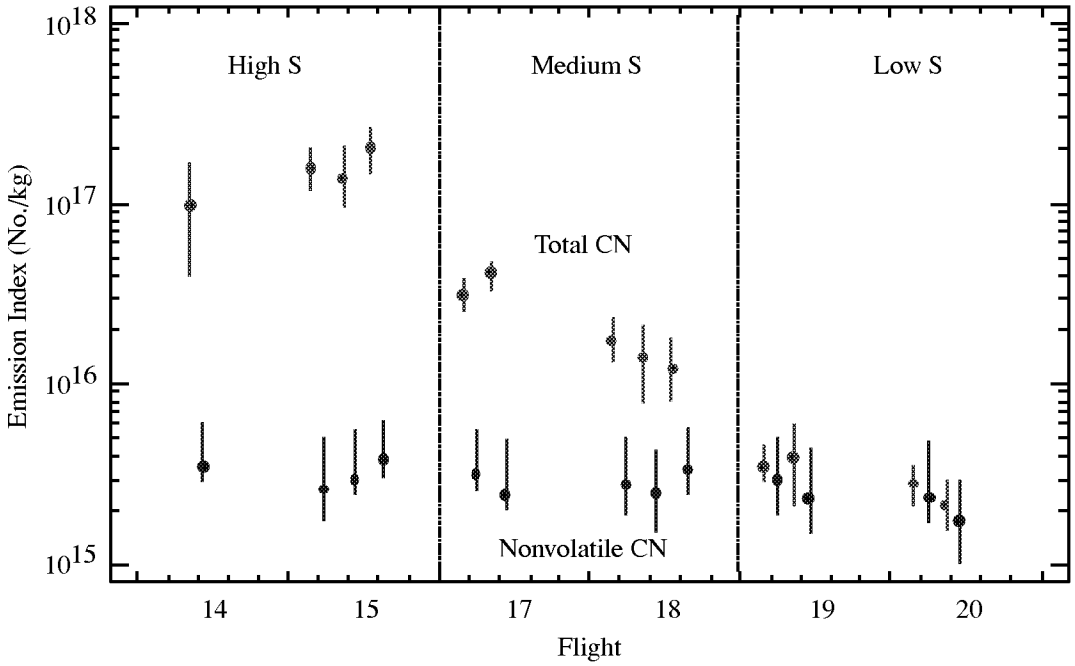

(a) Ultrafine.

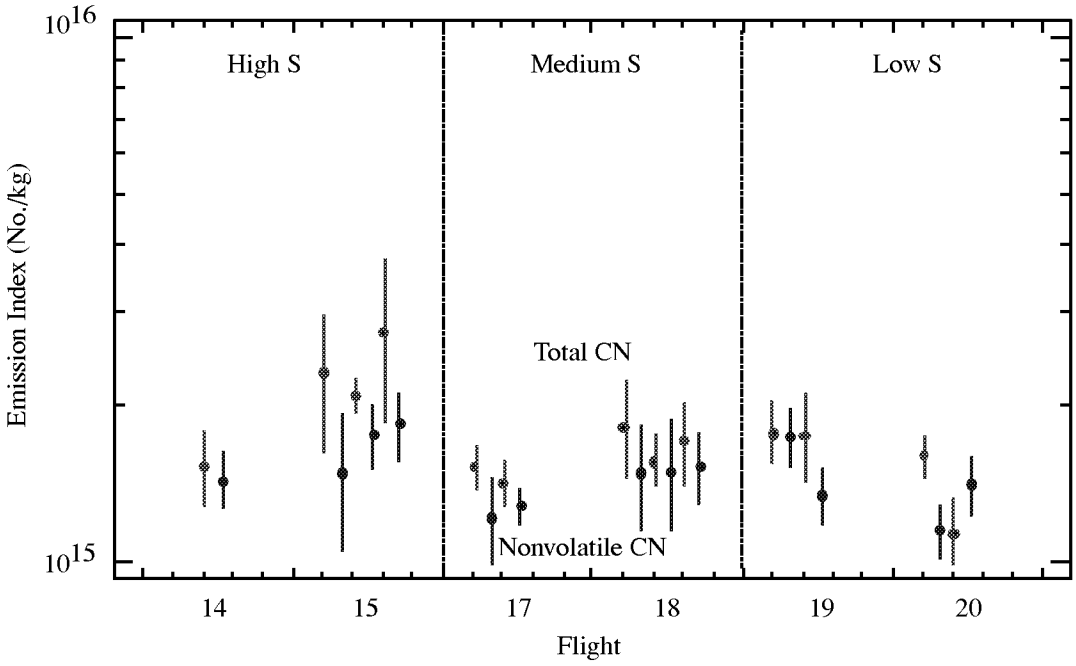

(b) Fine.

Figure 13. Aerosol emissions from the NJANG F-16 burning high, medium, and low S content fuels.

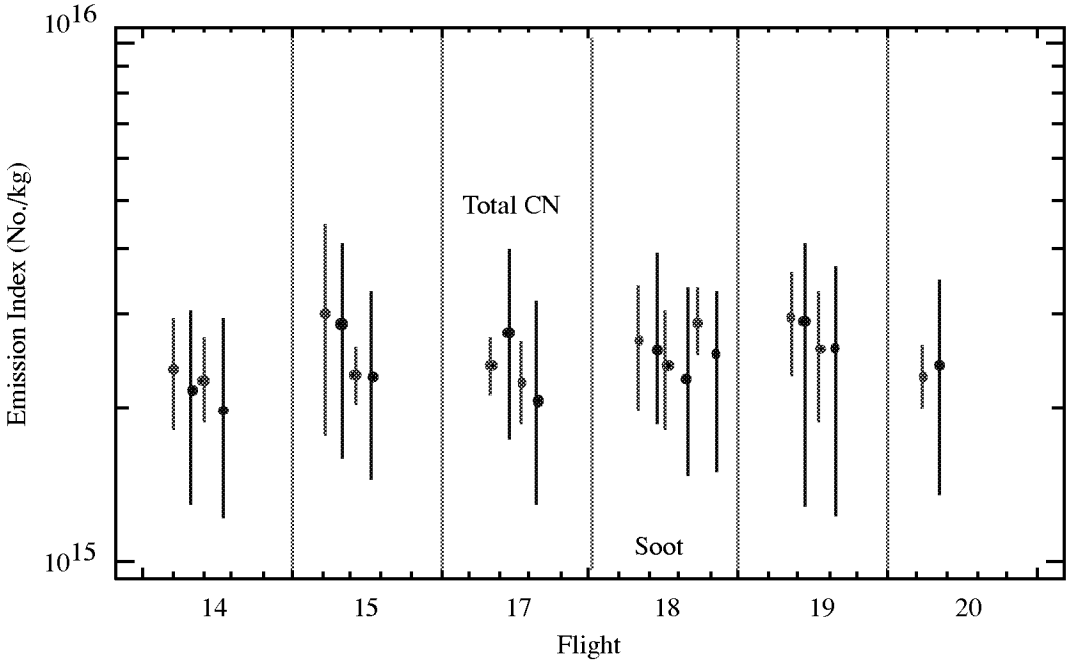

(a) Ultrafine.

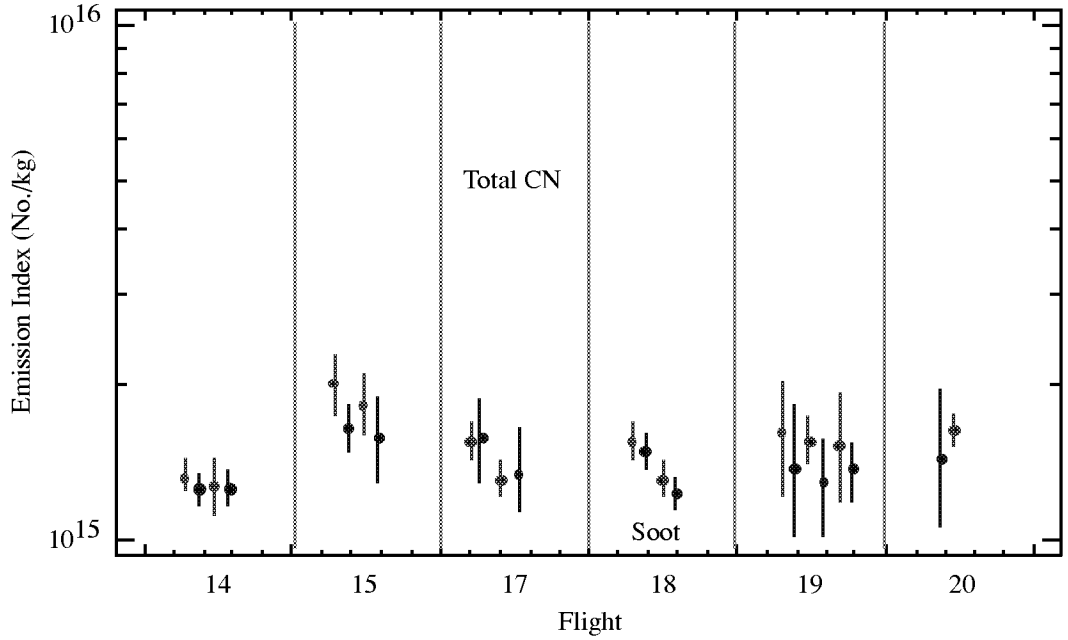

(b) Fine.

Figure 14. Aerosol emissions from the NJANG F-16 burning JP-8 fuel.

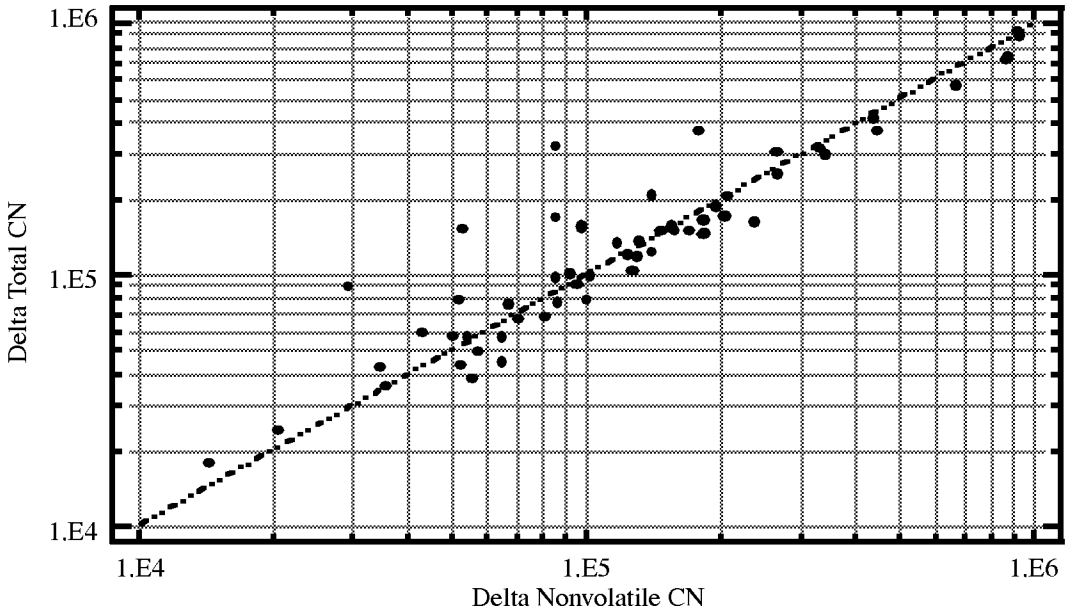

(a) Low S content fuel.

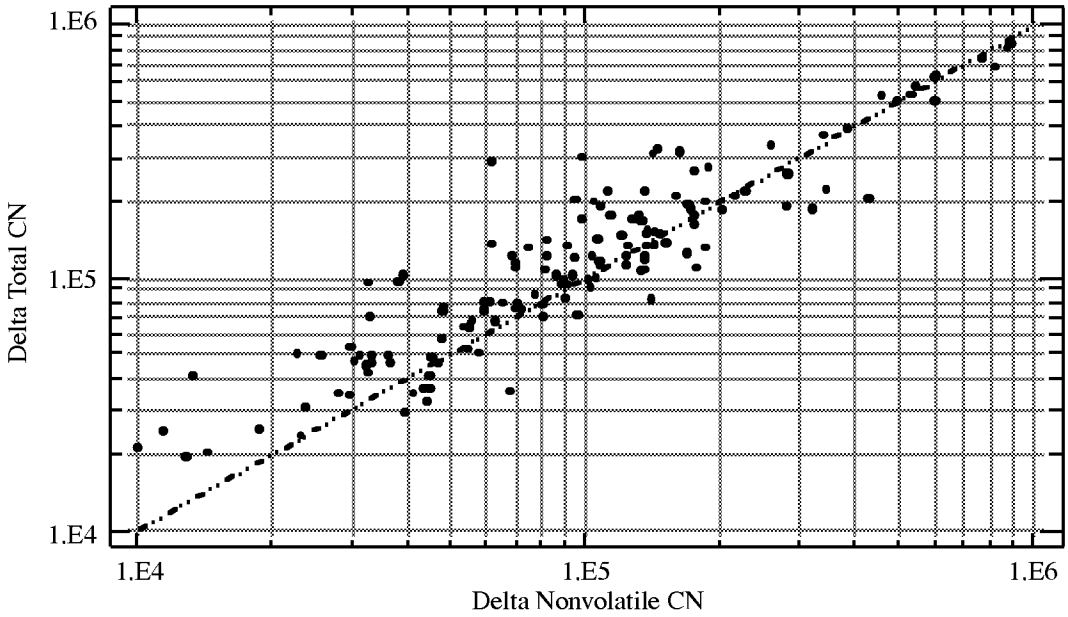

(b) JP-8 fuel.

Figure 15. Peak UF number densities within plumes from the aircraft plotted against peak NUF number densities.

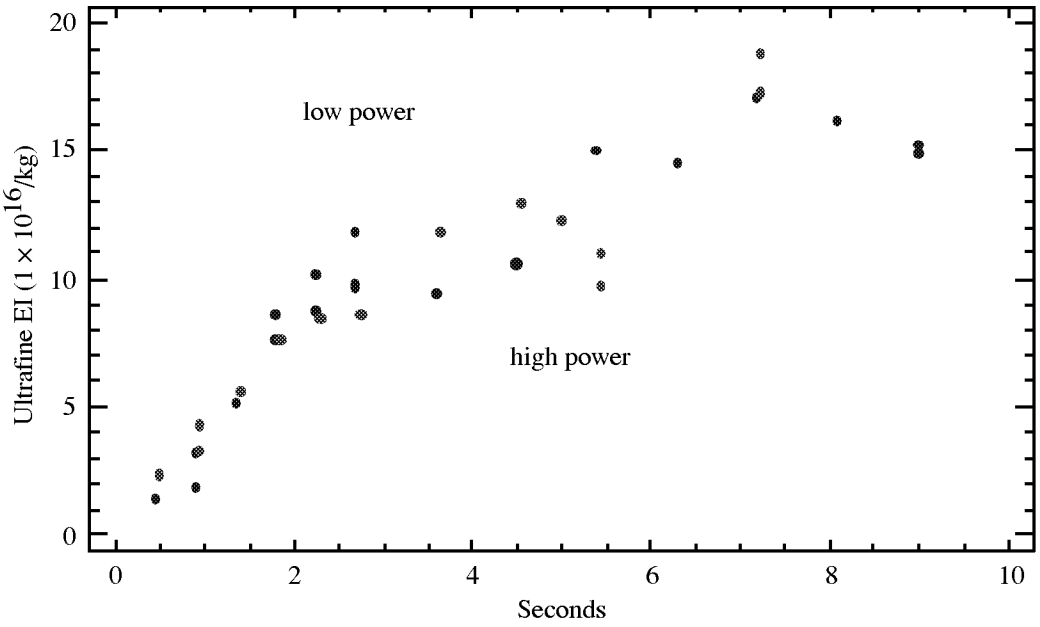

(a) High S fuel at altitude of 35000 ft.

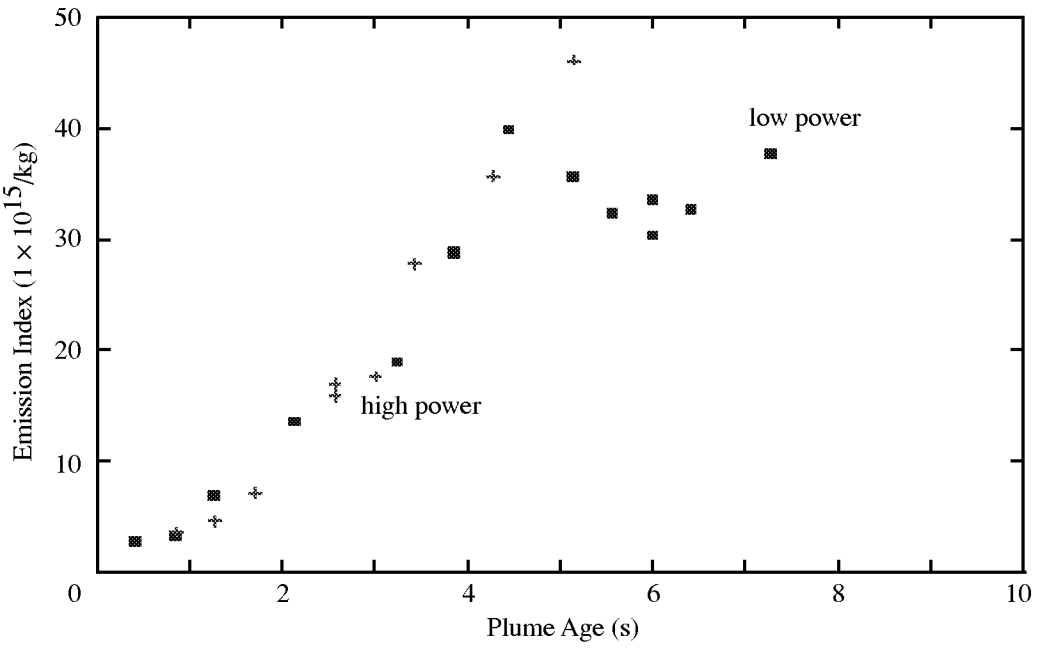

(b) Medium S fuel at altitude of 30000 ft.

Figure 16. NUF EI plotted versus plume age for the F-16.

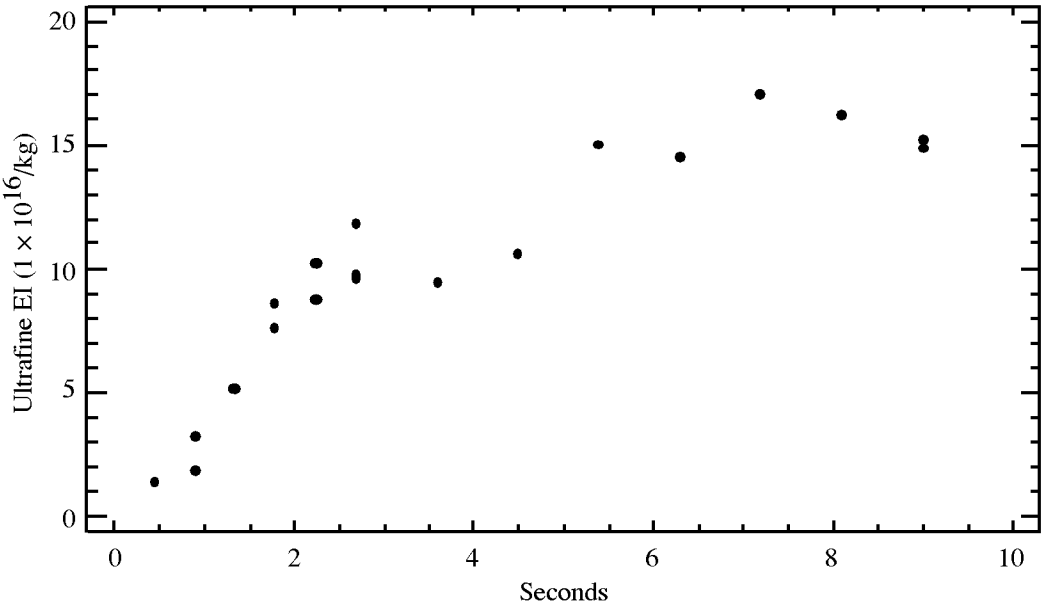

(a) High S fuel; low power; altitude, 35 000 ft.

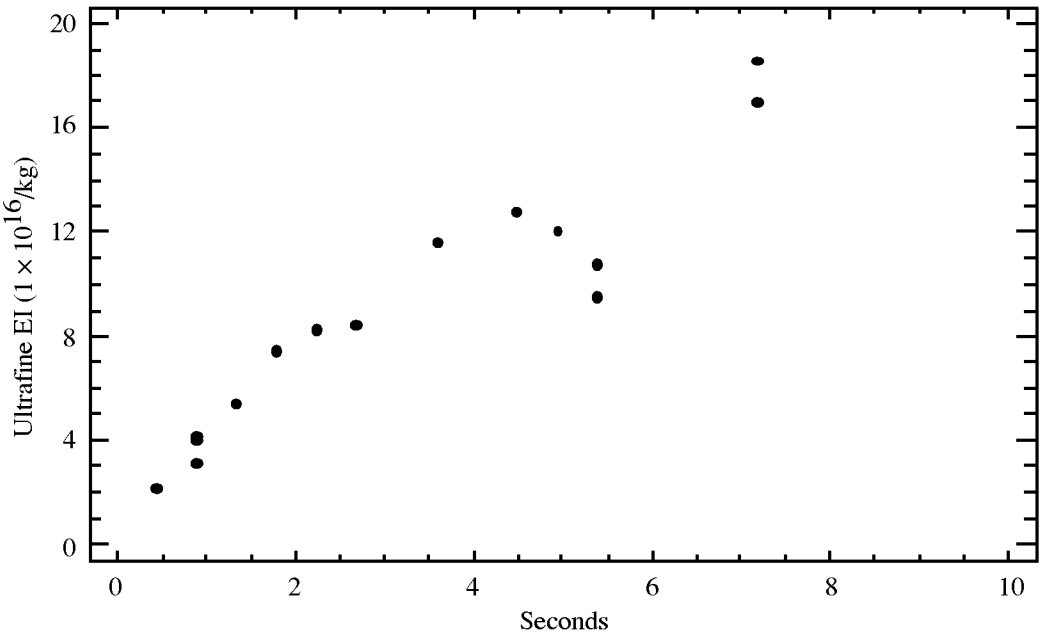

(b) High S fuel; high power; altitude, 35000 ft.

Figure 17. Plot of UF EI versus plume age for the F-16.

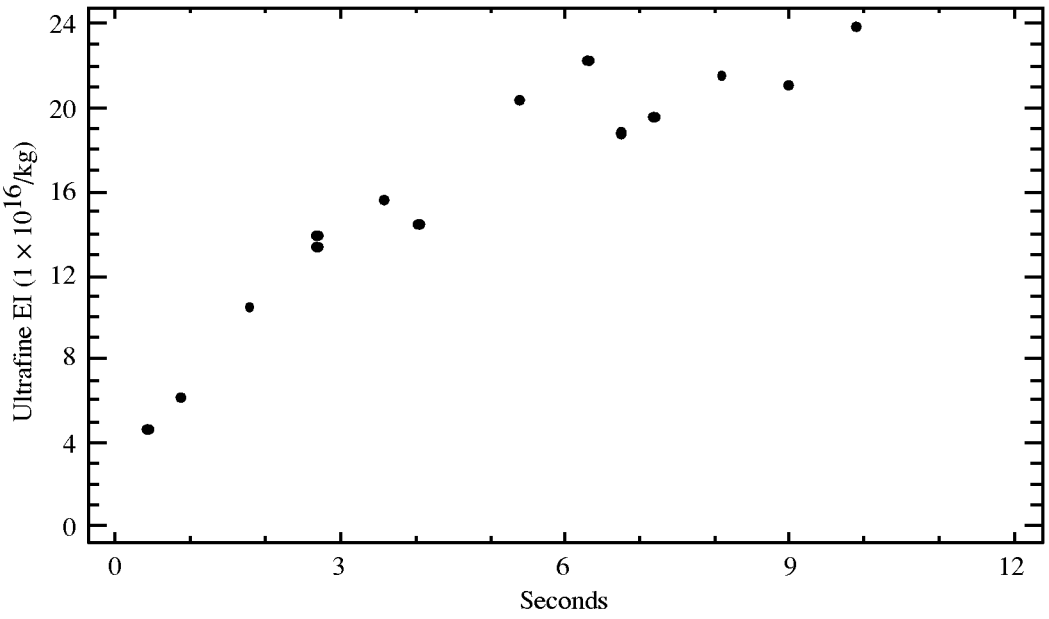

(c) High S fuel; high power; altitude, 38000 ft.

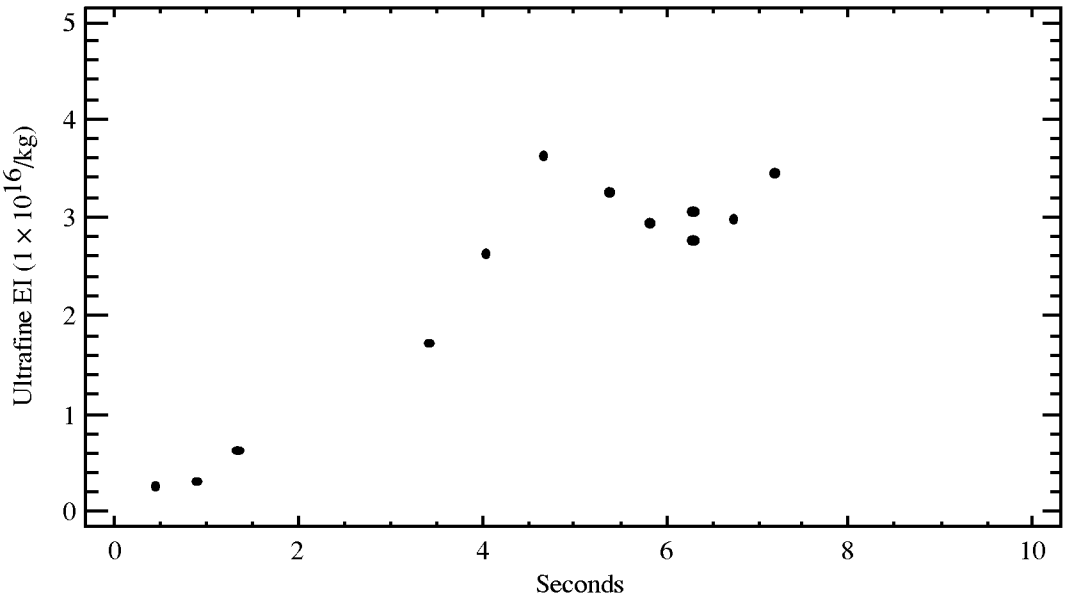

(d) Medium S fuel; low power; altitude, 30000 ft.

Figure 17. Continued.

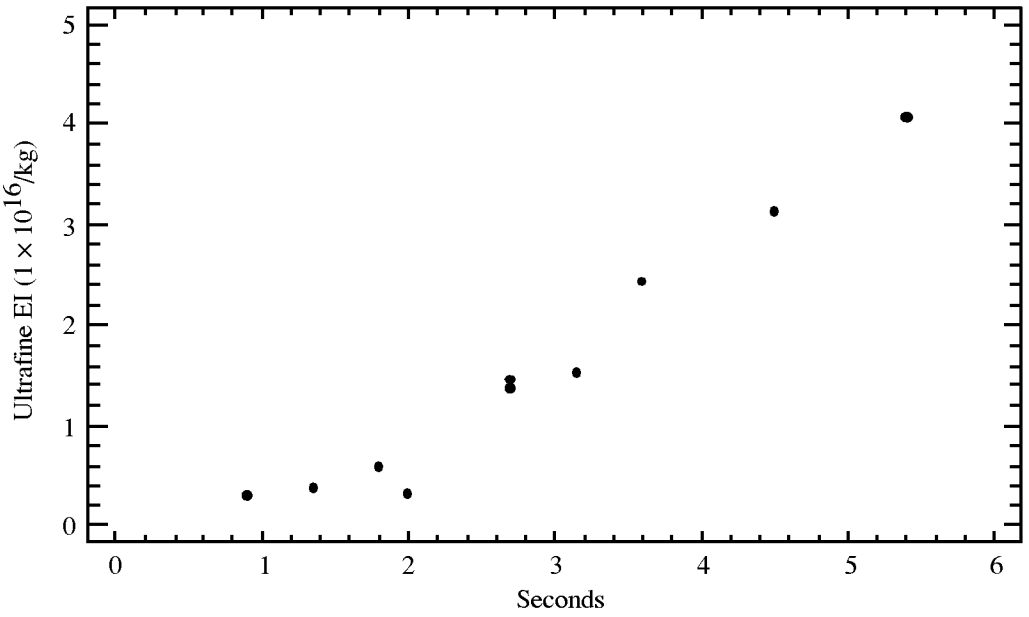

(e) Medium S fuel; high power; altitude, 30000 ft.

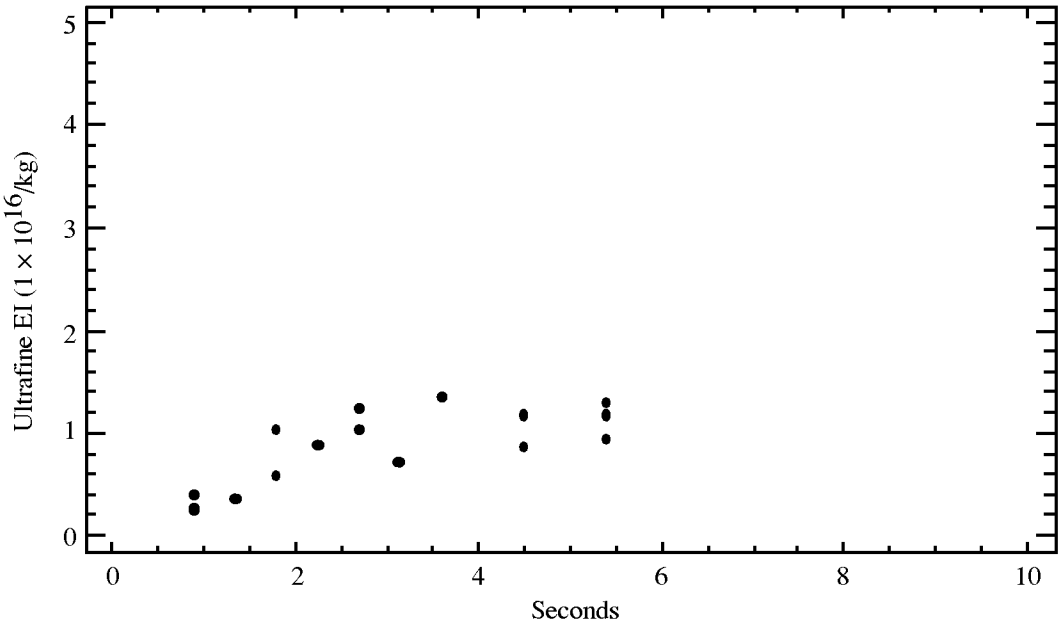

(f) Medium S fuel; high power; altitude, 35000 ft.

Figure 17. Continued.

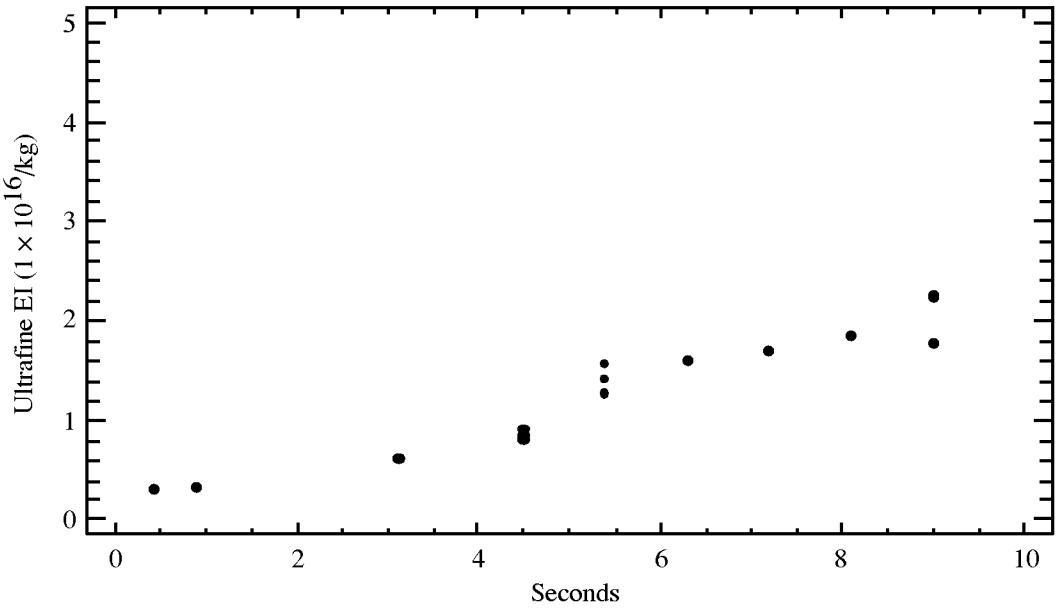

(g) Medium S fuel; high power; altitude, 35000 ft.

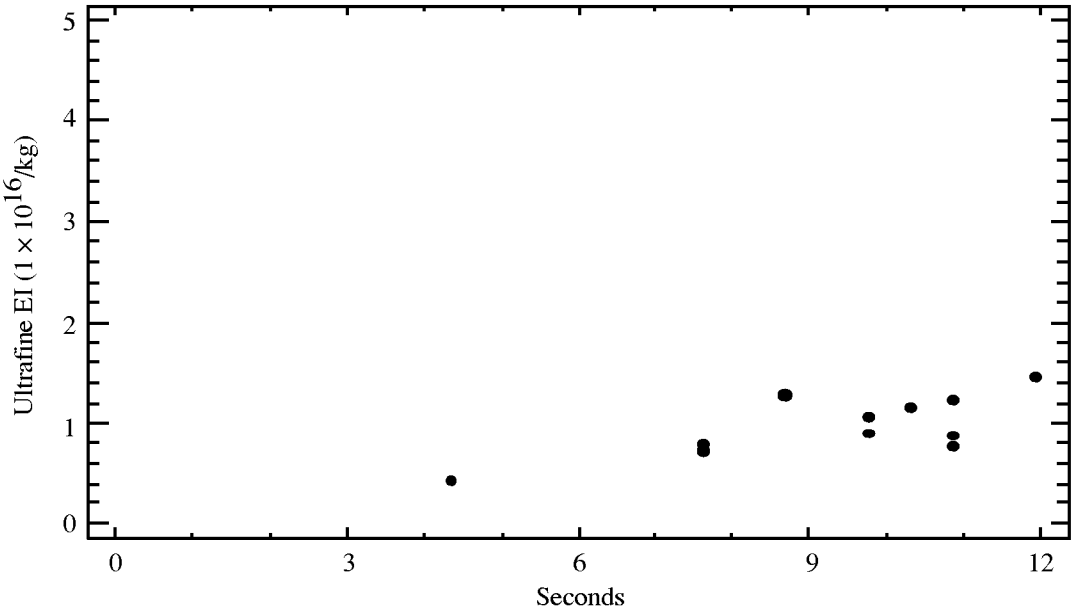

(h) Medium S fuel; high power; altitude, 37000 ft.

Figure 17. Concluded.

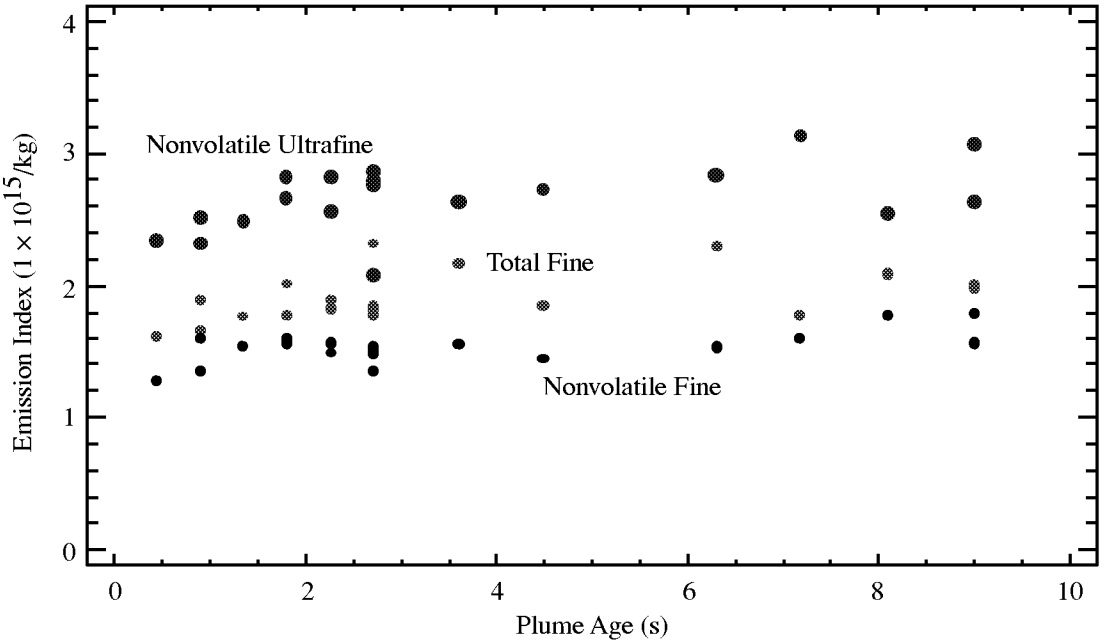

Figure 18. Plot of NUF, NF, and F EI's as a function of plume age.

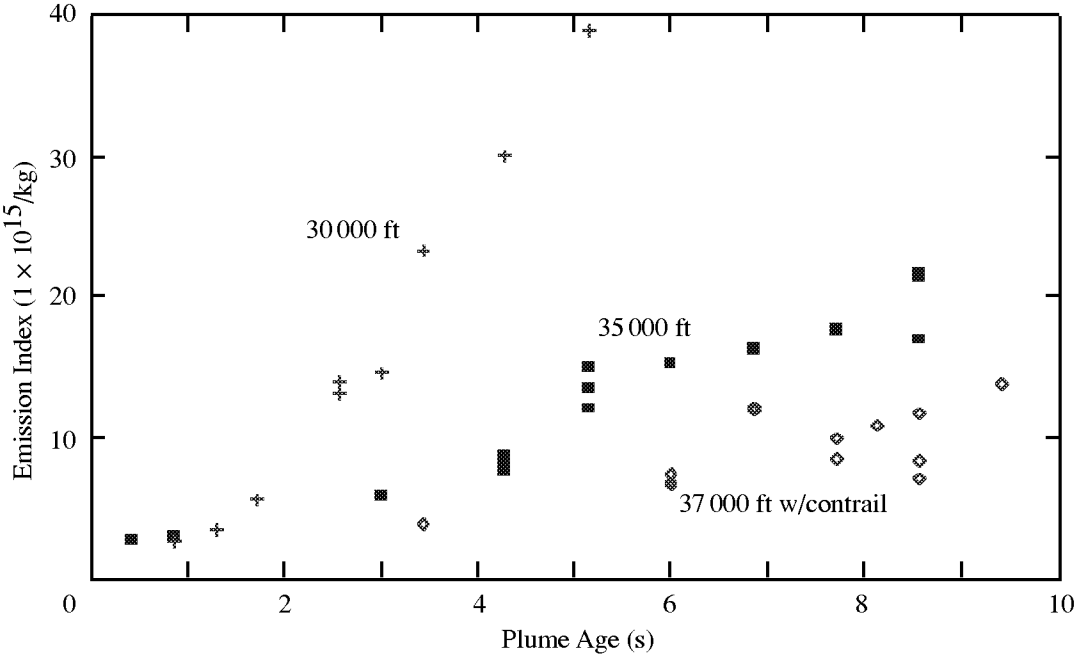

Figure 19. Plot of UF EI's as a function of plume age for the F-16 burning medium S fuel at high power.

REPORT DOCUMENTATION PAGE

Form Approved
OMB No. 07704-0188

1. AGENCY USE ONLY *(Leave blank)*	2. REPORT DATE	3. REPORT TYPE AND DATES COVERED
	March 1999	Technical Memorandum

4. TITLE AND SUBTITLE
Air Force F-16 Aircraft Engine Aerosol Emissions Under Cruise Altitude Conditions

5. FUNDING NUMBERS
WU 538-08-12-01

6. AUTHOR(S)
Bruce E. Anderson, W. Randy Cofer III, and David S. McDougal

7. PERFORMING ORGANIZATION NAME(S) AND ADDRESS(ES)
NASA Langley Research Center
Hampton, VA 23681-2199

8. PERFORMING ORGANIZATION REPORT NUMBER
L-17804

9. SPONSORING/MONITORING AGENCY NAME(S) AND ADDRESS(ES)
National Aeronautics and Space Administration
Washington, DC 20546-0001

10. SPONSORING/MONITORING AGENCY REPORT NUMBER
NASA/TM-1999-209102

11. SUPPLEMENTARY NOTES

12a. DISTRIBUTION/AVAILABILITY STATEMENT
Unclassified–Unlimited
Subject Category 45 Distribution: Standard
Availability: NASA CASI (301) 621-0390

12b. DISTRIBUTION CODE

13. ABSTRACT ***(Maximum 200 words)***

Selected results from the June 1997 Third Subsonic Assessment Near-Field Interactions Flight (SNIF-III) Experiment are documented. The primary objectives of the SNIF-III experiment were to determine the partitioning and abundance of sulfur species and to examine the formation and growth of aerosol particles in the exhaust of F-16 aircraft as a function of atmospheric and aircraft operating conditions and fuel sulfur concentration. This information is, in turn, being used to address questions regarding the fate of aircraft fuel sulfur impurities and to evaluate the potential of their oxidation products to perturb aerosol concentrations and surface areas in the upper troposphere. SNIF-III included participation of the Vermont and New Jersey Air National Guard F-16's as source aircraft and the Wallops Flight Facility T-39 Sabreliner as the sampling platform. F-16's were chosen as a source aircraft because they are powered by the modern F-100 Series 220 engine which is projected to be representative of future commercial aircraft engine technology. The T-39 instrument suite included sensors for measuring volatile and non-volatile condensation nuclei (CN), aerosol size distributions over the range from 0.1 to 3.0 μm, 3-D winds, temperature, dewpoint, carbon dioxide (CO_2), sulfur dioxide (SO_2), sulfuric acid (H_2S0_4), and nitric acid (HNO_3).

14. SUBJECT TERMS	15. NUMBER OF PAGES
Aircraft emissions; Aerosols; Soot particles; Sulfur emissions	58
	16. PRICE CODE: A04

17. SECURITY CLASSIFICATION OF REPORT	18. SECURITY CLASSIFICATION OF THIS PAGE	19. SECURITY CLASSIFICATION OF ABSTRACT	20. LIMITATION OF ABSTRACT
Unclassified	Unclassified	Unclassified	UL